



**NTNU – Trondheim**  
Norwegian University of  
Science and Technology

# Performance analysis of solar assisted R744 ground source heat pump in different climates

**Jingjing Ye**

Sustainable Energy

Submission date: December 2014

Supervisor: Trygve Magne Eikevik, EPT

Norwegian University of Science and Technology  
Department of Energy and Process Engineering



## MASTER THESIS

for

Student Jingjing Ye

Spring 2014

### **Solar assisted R744 ground source heat pump for buildings in different climates**

*Solar assistent R744 bergvarmepumpe for bygninger i annet klima*

#### **Background and objective**

One of the predominant alternative refrigerants for air conditioners in non-Article 5 countries which have almost completed the HCFC phase-out is R744. As the global energy crises and environmental problems become more and more serious, the ground source heat pump (GSHP) technology has shown a trend of booming growth. Whilst most non-Article 5 countries (under the Montreal Protocol) have for most of the time moderate temperate climates, many Article 5 countries experience extremely high or low ambient temperatures. This is considered to pose potential not very efficient performance when using GSHP only for the air conditioning. For this reason, many countries and enterprises are considering combing solar energy system to GSHP system to gain more feasibility and advantage for room air conditioners.

The work should address and compare the performance differences of solo R744 GSHP system and solar assisted R744 GSHP specifically at high or low ambient temperatures, using simulation by TRNSYS.

This project work will concentrate the activity for the solar assisted natural working fluid R744 in GSHP system. In the project there is a need to organize the rebuild of the test facilitates simulating model in TRNSYS. The building model has to be reinstalled with the solar assisted R744 GSHP system.

**The following tasks are to be considered:**

1. Literature review of the GSHP systems with natural working fluids in warm and cold climates, compared with non-natural refrigerant alternatives. (HCFC-22, HFC 410A, HFC 32)
2. Make a proposal for different operating schedules in the simulation model
3. Further development of the simulation model of a solar assisted GSHP system
4. Compare the energy efficiency calculated by simulation for solar assisted GSHP system applying R744 for different climates with GSHP like Haerbin, Beijing, Shanghai and Guangzhou
5. Write a scientific paper from the main results in the Master Thesis
6. Make proposal for further work

-- ” --

Within 14 days of receiving the written text on the master thesis, the candidate shall submit a research plan for his project to the department.

When the thesis is evaluated, emphasis is put on processing of the results, and that they are presented in tabular and/or graphic form in a clear manner, and that they are analyzed carefully.

The thesis should be formulated as a research report with summary both in English and Norwegian, conclusion, literature references, table of contents etc. During the preparation of the text, the candidate should make an effort to produce a well-structured and easily readable report. In order to ease the evaluation of the thesis, it is important that the cross-references are correct. In the making of the report, strong emphasis should be placed on both a thorough discussion of the results and an orderly presentation.

The candidate is requested to initiate and keep close contact with his/her academic supervisor(s) throughout the working period. The candidate must follow the rules and regulations of NTNU as well as passive directions given by the Department of Energy and Process Engineering.

Risk assessment of the candidate's work shall be carried out according to the department's procedures. The risk assessment must be documented and included as part of the final report. Events related to the candidate's work adversely affecting the health, safety or security, must be documented and included as part of the final report. If the documentation on risk assessment represents a large number of pages, the full version is to be submitted electronically to the supervisor and an excerpt is included in the report.

Pursuant to “Regulations concerning the supplementary provisions to the technology study program/Master of Science” at NTNU §20, the Department reserves the permission to utilize all the results and data for teaching and research purposes as well as in future publications.

The final report is to be submitted digitally in DAIM. An executive summary of the thesis

including title, student's name, supervisor's name, year, department name, and NTNU's logo and name, shall be submitted to the department as a separate pdf file. Based on an agreement with the supervisor, the final report and other material and documents must be given to the supervisor in digital format. All relevant data collected and produced during the project shall be delivered to the supervisor on a CD at the end of the project.

- Work to be done in lab (Water power lab, Fluids engineering lab, Thermal engineering lab)  
 Field work

Department of Energy and Process Engineering, January 14<sup>th</sup> 2014

---

Prof. Olav Bolland  
Department Head

---

Prof. Trygve M. Eikevik  
Academic Supervisor

Research Advisor:

Prof. Guoliang Ding, Shanghai Jiao Tong University, e-mail: [glding@sjtu.edu.cn](mailto:glding@sjtu.edu.cn)

Dr. Haitao Hu, Shanghai Jiao Tong University, e-mail: [huhaitao2001@sjtu.edu.cn](mailto:huhaitao2001@sjtu.edu.cn)

Dr. Armin Hafner, SINTEF Energi AS, e-mail: [armin.hafner@sintef.no](mailto:armin.hafner@sintef.no)

Prof. Natasa Nord, NTNU, e-mail: [natasa.nord@ntnu.no](mailto:natasa.nord@ntnu.no)

## **Acknowledgement**

This master thesis is my first attempt in master thesis. I'm very grateful the whole year in NTNU and the practice I gained from the project report.

I'd like to thank my supervisor Professor Trygve M. Eikevik, who offered generous suggestions and guidance when I needed help. He guided me to write one conference paper for GL2014. Mr. Laurent Georges also spent a lot of time discussing with me about the problems I met during the project, I appreciate his help a lot.

I'd also like to pay my greatest appreciation to Dr. Haitao Hu and Prof. Guoliang Ding for teaching me how to write a paper logically and persuasively. I finished two papers and one patent in Chinese with their guidance.

Courses held by Trygve M. Eikevik and Per O. Tjelflaat in NTNU have provided quite some information and knowledge that helps my project work, I thank them very much too.

## **Abstract**

As the world faces serious environmental and energy crisis, ground source heat pump stands out as an efficient air conditioning system which can supply both cooling and heating load for the building. Considering the environmental influence, R744, also known as CO<sub>2</sub> is chosen to be the working fluid.

However, when the ground source heat pump operates year after year in area without moderate climate, the system and soil suffers unbalance heat transfer. The soil temperature would go up in hot summer climate due to massive heat injection to earth and it would go down in cold winter climate because of substantial heat extraction from earth. This phenomenon would affect the heat transfer characteristics of underground heat exchanger, thus deteriorate the performance of the whole ground source heat pump system. A new way to improve present situation is in need.

In this thesis one possible solution was proposed. Using solar collector in cold winter climate area and air cooled gas cooler in hot summer climate area should help solve this problem. Solar collected heat remedies part of the lost heat in soil and air cooled gas cooler deliver part of the redundant heat to atmosphere.

In this thesis, a prediction model of the proposed system was developed. The numerical models of components like building, heat pump, underground heat exchanger, solar collector, hot water storage tank and air cooled gas cooler were developed and validated individually. Experimental data from existing literature were used to validate the models. The solar collector and water tank model get simulated results with less than 1°C deviation. The underground heat exchanger shows reliability more than 90%. The heat pump system model agrees very well with experimental results and air cooled gas cooler data has deviation less than 10%.

Based on the proposed model, this thesis studied the underground thermal balance, the investment cost and the operation cost of the system in different typical climate cities. The influence of assistant component on those issues was studied. The simulation results showed

that with solar collecting assistance, the unbalance rate of soil after one year can be reduced from 95.1% to 0.1% (in Trondheim, Norway). And with air cooled gas cooler, the unbalance rate of soil after one year can be reduced from 90.6% to 0.03% (in Guangzhou, China). When compared with solo R744 ground source heat pump, annual power needed decreased 41.5% (in Trondheim, Norway) in solar assisting system. Annual power needed is lower by 23% and investment cost is lower by 20% (in Shanghai, China) in air source gas cooler system.



## Sammendrag

Som verden står overfor alvorlige miljø- og energikrise, står bergvarmepumpe ut som en effektiv air condition-systemet som kan levere både kjøling og oppvarming belastning for bygningen. Tatt i betraktning den miljømessige påvirkning, R744, også kjent som CO<sub>2</sub> er valgt å være arbeidsmediet.

Men når bergvarmepumpe opererer år etter år i området uten moderat klima, systemet og jord lider ubalansevarmeoverføring. Jordtemperaturen ville gå opp i varmt sommerklima på grunn av massive varme injeksjon til jorden og det ville gå ned i kaldt vinterklima på grunn av betydelig varmeutvinningsextraction fra jorden. Dette fenomenet vil påvirke varmeoverføringsegenskaper av underjordisk varmeveksler, dermed forringe ytelsen til hele bergvarmepumpe system. En ny måte å forbedre dagens situasjon er inn.

I dette papir er en mulig løsning ble foreslått. Ved hjelp av solfanger i kaldt vinterklima område og luftkjølt gass kjøligere i varmt sommerklima området bør bidra til å løse dette problemet. Solar innsamlet varmerettsmidlerremedies del av den tapte varmen i jord og luftkjølte gasskjøler levere en del av den overflødig varme til atmosfæren.

I denne utredningen, ble en forutsigelse modell av det foreslåtte systemet utvikles. De numeriske modeller av komponenter som bygning, varmepumpe, underjordisk varmeveksler, solfanger, varmtvannstank og luftkjølte gasskjøler ble utviklet og validert individuelt. Eksperimentelle data fra eksisterende litteratur ble brukt for å validere modellene. Solfangeren og vanntank modellen får simulerte resultater med mindre enn 1 °C avvik. Den underjordiske varmeveksler viser pålitelighet mer enn 90%. Varmepumpesystemet modell enig veldig godt med eksperimentelle resultater og luftkjølt bensin kjøligere data har avvik lavere enn 10%.

Basert på den foreslåtte modellen, studert dette papiret den underjordiske termisk balanse, investeringskostnadene og driftskostnadene for systemet i forskjellige typiske klima byer. Påvirkningen av assistent komponent på disse spørsmålene ble studert. Simuleringsresultatene

viste at med solenergi innsamling assistanse, kan ubalansen frekvensen av jord etter ett år reduseres fra 95,1% til 0,1% (i Trondheim, Norge). Og med luftkjølte gasskjøleren cooler, kan ubalansen frekvensen av jord etter ett år reduseres fra 90,6% til 0,03% (i Guangzhou, Kina). Sammenlignet med solo R744 bergvarmepumpe, årlige kraftbehovet redusert 41,5% (i Trondheim, Norge) i solar bistå system. Årlige kraftbehovet er lavere med 23% og investeringskostnaden er lavere med 20% (i Shanghai, Kina) i luft kilde gasskjøler system.

## **Change to tasks**

Literature review of the GSHP systems with natural working fluids in warm and cold climates is done. There are some review about R744 heat pump system compared with non-natural refrigerant alternatives.

The proposal for different operating schedules in the simulation model is done in cold winter climate area as well as the hot summer climate area. The whole system with solar collecting system is proposed, air source gas cooler as additional model is also proposed.

Further development of the simulation model of a solar assisted GSHP system is done. The chosen cities are Harbin, Trondheim, Shanghai and Guangzhou. Beijing as one of the city that was analysed is given up because the unbalance rate is rather low and the situation is not very typical.

## Content list

Acknowledgement.....	4
Abstract .....	5
Sammendrag.....	7
Change to tasks.....	9
Content list .....	10
List of figures .....	12
List of tables .....	14
1. Introduction .....	15
2. Objectives.....	19
3. Literature review .....	20
3.1 History of CO <sub>2</sub> 's use as refrigerant.....	20
3.2 Unique properties of CO <sub>2</sub> as refrigerant .....	22
3.3 CO <sub>2</sub> transcritical cycle .....	25
3.4 CO <sub>2</sub> heat pump .....	28
3.4.1 Air source heat pump.....	28
3.4.2 Ground source heat pump .....	29
3.4.3 Heat pump water heater.....	30
3.5 Different kinds of solar assisted heat pump systems .....	30
4 System design and key performance indexes.....	33
4.1 System design.....	33
4.2 Key performance indexes.....	36

5	Mathematical modeling of the system .....	38
5.1	Heat pump model .....	38
5.2	Underground heat exchanger model.....	39
5.3	Solar collector model .....	41
5.4	Water storage tank model .....	41
5.5	Air cooled gas cooler.....	42
6.	Model validation .....	42
6.1	Heat pump model validation .....	42
6.2	Underground heat exchanger model validation.....	44
6.3	Solar collector and water storage tank model validation .....	46
6.4	Air cooled gas cooler model validation.....	48
7.	Performance simulation and economic analysis .....	49
7.1	Weather data and operation schedule .....	49
7.2	Simulation and analysis for solo R744 GSHP .....	51
7.3	Simulation and analysis for solar assisted R744 GSHP without heat injection .....	55
7.3.1	Simulation and analysis for Harbin’s case .....	55
7.3.2	Simulation and analysis for Trondheim’s case.....	56
7.4	Simulation and analysis for solar assisted R744 GSHP with heat injection .....	57
7.4.1	Simulation and analysis for Harbin’s case .....	57
7.4.2	Simulation and analysis for Trondheim’s case.....	59
7.5	Simulation and analysis for R744 GSHP with air cooled gas cooler.....	61
7.5.1	Simulation and analysis for Shanghai’s case.....	61
7.5.2	Simulation and analysis for Guangzhou’s case.....	64
8.	Conclusion.....	66
9.	Proposal for further work .....	68
	Reference.....	69

## List of figures

Fig. 1 Transcritical CO <sub>2</sub> cycle in a pressure-enthalpy diagram.....	26
Fig. 2 Whole system schematic diagram.....	34
Fig. 3 System schematic diagram in cooling mode in hot summer area.....	35
Fig. 4 System schematic diagram in heating mode in cold winter area.....	35
Fig. 5 System schematic diagram in charging mode in cold winter area.....	36
Fig. 6 Single control volume segment of gas cooler.....	39
Fig. 7 Measured and modeled results of temperature change.....	43
Fig. 8 Measured and modeled results of temperature change without low flow data.....	44
Fig. 9 Schematic diagram of theoretical model.....	45
Fig. 10 Experimental and modeled data of heat transfer between heat exchanger and soil .....	45
Fig. 11 Experimental and simulated value of soil temperatures.....	46
Fig. 12 Tank average temperature comparison, day 1.....	47
Fig. 13 Tank average temperature comparison, day 2.....	47
Fig. 14 Ambient temperature of Harbin.....	50
Fig. 15 Ambient temperature of Trondheim.....	50
Fig. 16 simplified system schematic of solo R744 GSHP.....	51
Fig. 17 Performance of SAGSHP in Harbin (without heat injection).....	55
Fig. 18 Performance of SAGSHP in Trondheim (without heat injection, Norwegian style) .....	56
Fig. 19 Performance of SAGSHP in Harbin (with heat injection).....	58
Fig. 20 Heat exchange distribution with SAGSHP in Harbin.....	59

Fig. 21 Performance of SAGSHP in Trondheim (with heat injection, Norwegian structure)	59
.....	
Fig. 22 Performance of SAGSHP in Trondheim (with heat injection, Chinese structure)	60
.....	
Fig. 23 Heat exchange distribution with SAGSHP in Trondheim (Norwegian structure)	61
Fig. 24 Heat exchange distribution with SAGSHP in Trondheim (Chinese structure)....	61
Fig. 25 Performance of GSHP with gals cooler in Shanghai .....	62
Fig. 26 Heat exchange distribution of GSHP with air cooled gas cooler in Shanghai.....	63
Fig. 27 Performance of GSHP with gals cooler in Guangzhou.....	65

## List of tables

Table 1 GWP value of different refrigerants .....	17
Table 2 CO <sub>2</sub> thermodynamic properties around critical point.....	24
Table 3 Correlations to optimize discharge pressure.....	26
Table 4 Comparisons of several novel CO <sub>2</sub> transcritical cycles.....	27
Table 5 Ground source heat exchanger parameter .....	40
Table 6 Experimental data of air cooled gas cooler .....	48
Table 7 Operation schedule of different cities.....	51
Table 8 Energy loads of solo GSHP system in Harbin.....	52
Table 9 Energy loads of solo GSHP system in Trondheim .....	53
Table 10 Energy loads of solo GSHP system in Shanghai .....	53
Table 11 Energy loads of solo GSHP system in Guangzhou.....	54
Table 12 Comparisons of operation in solo GSHP and GSHP with air source gas cooler .....	64
Table 13 Comparisons of investment in solo GSHP and GSHP with air source gas cooler .....	64
Table 14 Comparisons of operation in solo GSHP and GSHP with air source gas cooler .....	65



## 1. Introduction

One recent report<sup>[1]</sup> proposed by the USA Department of Energy showed that the global energy consumption in 2020 would be more than twice of the present level according to the current tendency. Such an increasing energy requirement will aggravate energy shortage and environment pollution. Reducing the consumption of energy is as important as finding the environmental friendly refrigerant nowadays. Since about 40% of the energy is consumed by buildings, and more than half of the building energy consumption is caused by the air conditioning system, it is crucial to find a way to make our air conditioning system more efficient.

GSHP systems can operate better to achieve high energy efficiency especially in some areas where heating and cooling loads of buildings are well balanced all year round because of the long-term transient heat transfer in the ground heat exchangers. If the system is installed in some moderate-climate location, the COP of GSHP system can reach as high as some point between 3 and 4. This figure is 20 percent to 30 percent higher than that of the conventional air source heat pump (ASHP) systems. However, when viewing the system heat transfer on annual base, most buildings in warm-climate or cold-climate regions have unbalanced loads, dominated by rather cooling loads or heating loads. For example, when GSHP systems is installed in some heating dominated buildings in cold-climate area, more heat will be extracted from ground than that is rejected to the ground every year around. If this situation continues, the ground soil temperature will become lower than original average soil temperature, which will affect the heating transfer performance of the borehole, and moreover, the system performance over time. To reduce the influence that will be made to the ground temperature, the installation of GSHP systems often demand larger ground heat

exchangers, which may be restricted by the construction sites and the initial cost<sup>[2]</sup>. To make the GSHP more suitable for widely utilization, one way is to decrease the initial cost of the GSHP, another alternative way is to find some way to improve the system performance by combining integrated approaches in the design of GSHP systems.

Though there have been a lot of researches about how to improve the system performance in the design of GSHP systems, fewer researches have focused on the imbalance of the ground heat on annual base. According to existed researches, the most common way is to change the system design method to adapt the system to local climate. For cooling-dominated buildings, there has been utilization of cooling towers in the buildings to reduce the imbalance<sup>[3]</sup>. Another proposal is an effective method to decrease the imbalance and use energy efficiently by using heat recovery technologies and optimizing the set value of indoor temperature<sup>[4]</sup>. For heating dominated buildings the researches are mostly focused on combining solar energy<sup>[5]</sup>, but most of them pay less attention to the imbalanced ground energy, and the refrigerants used in the mentioned existing research are conventional refrigerants like R134a.

Due to the harms that can be done to the global environment by chlorofluorocarbons (CFCs) and hydrochlorofluorocarbons (HCFCs), Montreal Protocol signed in 1987 made a successful progress by eliminating the application of CFCs in new refrigeration equipment until 1996 in most developed countries, and completed the elimination until 2010 in many developing countries. The most recent meeting of the Montreal Parties<sup>[6]</sup> in September 2007 agreed to accelerate the phase-out of HCFCs in non-Article 5(1) countries according to the following schedule: 75% by 2010; 90% by 2015; 99.5% during the period 2020–2030; and complete phase out as of 2030. In 2003 and 2004, reported consumption levels were 40% and 30% of baseline, respectively. In Article 5(1) countries, use of HCFCs can continue to expand prior to a 2013 freeze; full phase out is scheduled for 2040 with phase out steps of 10% by 2015; 35% by 2020; 67.5% by 2025; and an annual average of 97.5% during 2030–2040. Reductions of Hydrofluorocarbons (HFCs), such as R134a, are already undertaken by Parties to the Montreal Protocol amount to significant cuts in direct (non-energy related) greenhouse effects, due to their high GWP values. The European Union already approved the scheduled phase-out of mobile air conditioning systems using refrigerants with GWP higher than 150.

Hence, the research about utility of natural refrigerant is becoming a hot spot in recent

years. CO<sub>2</sub> is considered one of the most potential refrigerants since its zero impact on the ozone layer and Global warming potential (GWP) is 1, which is a significant advantage compared with many other refrigerants used nowadays (Table 1). It is also non-flammable and non-toxic. Thanks to the low critical temperature of CO<sub>2</sub>, the condensing process is working above the critical pressure and the evaporating process is working below the critical pressure, thus the unique CO<sub>2</sub> cycle is called transcritical cycle. In the transcritical cycle CO<sub>2</sub>, heat rejection takes place at supercritical pressures and temperatures. Unlike a conventional CO<sub>2</sub> refrigeration cycle, the transcritical cycle does not suffer capacity and efficiency losses at high heat rejection temperatures<sup>[7]</sup>. Besides the advantages of CO<sub>2</sub> mentioned above, it has more favorable features for example, it is compatible with normal lubricants and common machine construction materials, it is low-cost and has wide availability, the pressure ration of the cycle is much lower and the heat transfer is quite good.

Still, the utility of CO<sub>2</sub> as substitute refrigerant in practical heating, ventilation, air conditioning and refrigeration systems is restrained by its high working pressure, lower COP caused by huge expansion loss compared to conventional refrigerants and other factor like non-matching working components.

Developments and advances in CO<sub>2</sub> technology in recent years are reviewed in this thesis. History of CO<sub>2</sub> is elaborated, cycle modifications aiming at improving the working efficiency of CO<sub>2</sub> cycle are looked into, special requirements for working components and difference applications are also discussed.

**Table 1 GWP value of different refrigerants**

Refrigerant	CO <sub>2</sub>	Ammonia	R134a	R22	R407c	R410a	R404a
GWP	1	0	1300	1700	1610	1725	3260

When CO<sub>2</sub> is used in air conditioning system, unlike a conventional CO<sub>2</sub> refrigeration cycle, the transcritical cycle does not suffer capacity and efficiency losses at high heat rejection temperatures<sup>[8]</sup>. There have been studies of the performance of a direct-expansion geothermal heat pump using CO<sub>2</sub>, in which the refrigerant flows inside horizontal ground source heat exchanger. In the megacities, the building energy is much larger than that provided by direct-expansion geothermal heat pump, and vertical heat exchanger is preferred to decrease the

needed ground surface<sup>[9]</sup>, which gives good guidance to the design of the solar assisted CO<sub>2</sub> ground source heat pump system.

## 2. Objectives

Considering both the use of natural refrigerant CO<sub>2</sub> and the change of soil temperature after annual operation of ground source heat pump, it is essential propose and simulate a novel system. This system should contain a ground source heat pump using CO<sub>2</sub> as working fluid, and other assistant components to assure the balance of heating and cooling load. The novel system should be able to satisfy the cooling need and the heating need for a building. In this thesis, the system uses auxiliary solar collecting system to supply part of the heating need in winter, to reduce the quantity of heat extracted from earth. The system also uses air source gas cooler to release part of the heat to the atmosphere rather than the soil. In this way, the system will suit area with unbalance heating and cooling load without causing soil temperature change.

The work in this thesis will design the system and develop different numerical models for every component. By combining building model, solar collector model, water tank model, gas cooler model, heat pump model, underground heat exchanger model and other models together, the system model is assembled and simulated. The model is validated by experimental data from existing literature.

In the results, this thesis will address and compare the performance differences of solo R744 GSHP system, solar assisted R744 GSHP without heat injection in summer, solar assisted R744 GSHP with heat injection in summer specifically at low ambient temperatures. It will also will address and compare the performance differences of solo R744 GSHP system, gas cooler assisted R744 GSHP specifically at high ambient temperatures. System model is simulated in TRNSYS.

### **3. Literature review**

#### **3.1 History of CO<sub>2</sub>'s use as refrigerant**

The first pioneering researchers in the world who made the CO<sub>2</sub> as a refrigerant possible were two Scottish physicians, Dr. William Cullen and Dr James Black. Black's discovered CO<sub>2</sub> by the experiments of heating magnesium carbonet, at that time, he called CO<sub>2</sub> as 'fixed air'. After his discovery, CO<sub>2</sub> is proved to be existing in many human being and natural behaviors, such as breathing and firing. Black was right about that CO<sub>2</sub> will be in the air in small quantities, as we know now it takes 0.03% of the atmosphere. But during that time neither Cullen nor Black connected CO<sub>2</sub> to refrigeration, let alone thought about using it as refrigerant. Only after about 100 years started the ideas about CO<sub>2</sub> can be used as a refrigerant.

CO<sub>2</sub> was first proposed as a refrigerant by Alexander Twinning in a British patent in 1850. There was one shared blemish for all the different early refrigerants. Even though the design concept was good, the industry was not capable of manufacturing the required components at that time. As a result, the development of the refrigeration system was unstable because every novel design relies on the synchronous and qualified advances in related areas<sup>[10]</sup>.

CO<sub>2</sub> refrigeration embraced its first breakthrough thanks to the American self-taught scientist Thaddeus Lowe in Texas. Lowe who served as an observer in American Civil War developed a compressor for filling military observation balloons with hydrogen in 1860. With further experiments with CO<sub>2</sub>, Lowe adapted his compressor for CO<sub>2</sub> using, and used the compressor to produce man made ice. This system is 20 years before other developments in CO<sub>2</sub> systems, and Lowe revealed a closed vapor compression cycle including compressor, condenser and evaporator in his British patent number 952 in 1867. Lowe started working to use CO<sub>2</sub> refrigeration to ship frozen beef by sea on a board ship from Texas to New Orleans in 1869.

C. Linde built the first CO<sub>2</sub> compression refrigeration system in Europe, 1881. In 1886 Franz Windhausen got the patent of his improved CO<sub>2</sub> compressor, which was further improved

in 1889 by Everard Hesketh of J&E Hall. A compound CO<sub>2</sub> compressor with higher efficiency was then developed. CO<sub>2</sub> became one popular choice for larger systems thanks to the sufficiently improvement promoted by those pioneer.

The booming of CO<sub>2</sub> as a refrigerant, especially in commercial side, the pioneering CO<sub>2</sub> companies in early years should take the credit. In 1897 Kroeschell Bros. Ice Machine Company was founded in Chicago by the Kroeschell Bros. Boiler Company. It produced CO<sub>2</sub> compressors, condensers, water and brine coolers, high-pressure CO<sub>2</sub>, valves and fittings for cold storage systems. Fred Wittenmeier built another CO<sub>2</sub> refrigeration machine company making horizontal, double-acting compressors in Chicago. Later in the 1930s, the company became a refrigeration contractor. There are also other companies manufacturing CO<sub>2</sub> system equipment including the Carbondale Machine Company in Pennsylvania and the American Carbonic Machinery Company<sup>[11]</sup>.

However, with the beginning of 1930s, since the ammonia's most concern-safety issues were largely solved by progressed manufacture levels, ammonia began to take CO<sub>2</sub>'s place in industrial refrigeration. Additionally, with the introduction of new synthetic refrigerants like CFCs and HCFCs, CO<sub>2</sub> did not survive from the competition. According to the registration of marine refrigeration records in London, CO<sub>2</sub> systems gradually phased out from 1950 until 1960<sup>[12]</sup>.

Around 1990, the public started to pay attention to the ozone depleting ability that CFCs and HCFCs have. As Montreal Protocol executed to phase them out, the decline of CFCs and HCFCs caused an enormous rise in searching for the new refrigerant. CO<sub>2</sub>, as a natural and old refrigerant, was viewed as a concrete alternative.

Professor Gustav Lorentzen patented an application for a transcritical CO<sub>2</sub> system for automotive air-conditioning in 1990<sup>[13]</sup>. In 1991 Dr Forbes Pearson published patents about using CO<sub>2</sub> as a fugitive secondary refrigerant, including a novel hot gas defrost system in Britain, France, Germany and the USA<sup>[14]</sup>. In 1993, Lorentzen and Pettersen investigated an automotive air conditioning system using a transcritical CO<sub>2</sub> cycle<sup>[15]</sup>. Soon the trend became wider, from 1994 to 2004, the number of papers on CO<sub>2</sub> in the Gustav Lorentzen conference grew from 6 to 50, more studies appeared, including CO<sub>2</sub> cascade refrigeration and heat pump water heaters, for which transcritical operation makes it possible to adapt very well to the

gliding temperature heating demand required for tap water<sup>[16]</sup>. Till now, there has been study and application in “all-CO<sub>2</sub>” supermarket in Italy<sup>[17]</sup>, CO<sub>2</sub> heat pump space heating system<sup>[18]</sup> and the scope keeps growing wider so far.

### **3.2 Unique properties of CO<sub>2</sub> as refrigerant**

CO<sub>2</sub>, as an ideal refrigerant, it is special for its high specific heat, high volumetric heat capacity and a lot other excellent thermodynamic and transport properties. But it is unique because of the low critical temperature. The temperature and pressure at the critical point are 303.97K and 7.353MPa, respectively. P. Bansal<sup>[19]</sup> did a review about CO<sub>2</sub> as a low temperature refrigerant. CO<sub>2</sub> possesses excellent thermoophysical properties at low temperatures that are quite different from other refrigerants. At a given saturation temperature and pressure, the surface tension, the liquid viscosity and ratio of liquid to vapor density of CO<sub>2</sub> are different from other refrigerants, such as R717, R22, R410A and R134a. With lower density ratio of liquid to vapor, CO<sub>2</sub> velocity changes less and the two-phase Reynolds number is smaller when the mass flow rate during the boiling process is the same. This feature makes CO<sub>2</sub> more suitable for the direct expansion type evaporators since the two-phase distribution is better. At the same time, lower liquid viscosity enables CO<sub>2</sub> of smaller pressure losses compared with other refrigerants. From around -60 °C till around 0 °C, the pressure of CO<sub>2</sub> can rise from lower than 1 MPa to almost 4MPa, such a small temperature change along with the pressure growing, this also assures CO<sub>2</sub> good two-phase distribution inside heat exchangers<sup>[20]</sup>.

Another advantage of CO<sub>2</sub> as a refrigerant is that it is not like other refrigerants that have to operate at sub-atmospheric pressures at low temperatures, which would bring phase separation and oil management problems into the system because of the low velocities. Hence CO<sub>2</sub> is a good choice of refrigerant in two-phase boiling and condensation applications regarding the higher liquid and vapour thermal conductivities and the lower liquid viscosity and surface tension. CO<sub>2</sub> also has the highest volumetric refrigeration capacity amongst when compared with other refrigerants at low temperature, which is the benefit from its relatively lower specific volume. That feature makes smaller-size compressors for the same operating conditions



possible.

Pressures in CO<sub>2</sub> systems are typically 5 to 10 times higher than those with conventional refrigerants, so the safety concern about CO<sub>2</sub> refrigerant is essential in system design and operating<sup>[21]</sup>. In most cases, they require more complex pressure relief systems that can be isolated. Besides, high pressure gas/liquid CO<sub>2</sub> can be violent and fatal, if CO<sub>2</sub> concentration in the air exceeds 5%, there is a danger of breathing difficulties which ends with unconsciousness. That's why there is always demand for designs in the system to prevent CO<sub>2</sub> from directly going into the atmosphere to harm people in occupied spaces. The system also needs complementary controlling components such as detectors and high and low pressure alarms to ensure safety in operation as CO<sub>2</sub> in the air can't be noticed by eyes or noses for its odorlessness and colorlessness.

Since the critical temperature is so easily reached, the heat rejection temperature is mostly higher than the critical temperature of CO<sub>2</sub>. Simultaneously, the heat absorption process takes place below the subcritical area, this operating cycle is called transcritical cycle. As the working fluid during condensing process is under a supercritical pressure thus there is no phase change, the heat exchanger where the heat rejection appears is named gas cooler rather than condenser in the conventional subcritical systems.

While there is no phase change in supercritical status, the supercritical fluids near the critical point exhibits large variations in thermophysical properties such as the thermal conductivity, the viscosity, the specific heat, and the density with the change of temperature. This area where these phenomena are observed is called the pseudocritical region and special point at a given pressure, the temperature of when the specific heat reaches a peak is named the pseudocritical point.

The pseudocritical temperature  $T_{pc}$  of CO<sub>2</sub> as function of pressure can be best fitted by the following algebraic equation<sup>[22]</sup>:

$$T_{pc} = -122.6 + 6.124p - 0.1657p^2 + 0.01773p^{2.5} - 0.0005608p^3, \quad (1)$$

where the pseudocritical temperature  $T_{pc}$  is in °C and the pressure  $p$  is in bar. It follows that  $T_{pc} = 34.6$  °C at  $p = 80$  bar and  $T_{pc} = 45.0$  °C at  $p = 100$  bar.

Span and Wagner in 1996<sup>[23]</sup> developed a new equation of CO<sub>2</sub> in form of Helmholtz energy as:

$$\frac{A(\rho, T)}{(RT)} = \phi(\delta, \tau) = \phi^o(\delta, \tau) + \phi^r(\delta, \tau), \quad (2)$$

The dimensionless Helmholtz energy  $\phi$  is defined as  $\phi = A/(RT)$ , where  $R$  is the gas constant and  $T$  is the thermodynamic temperature.

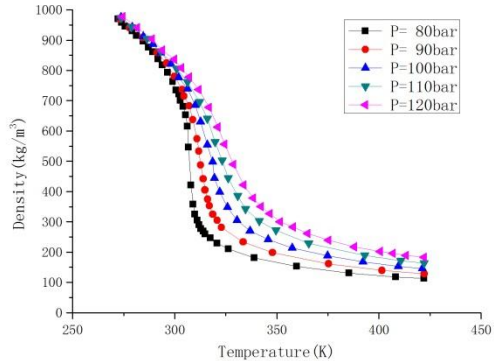
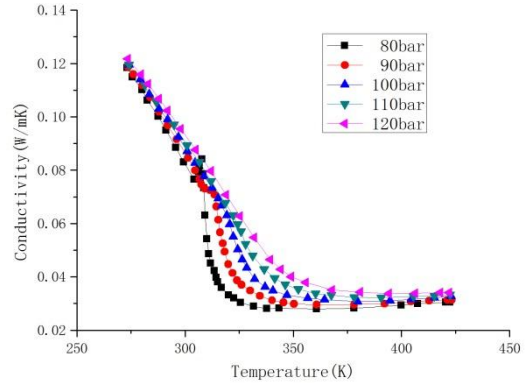
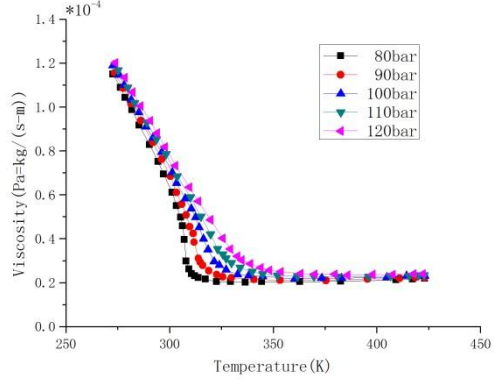
And according to the results of Vesovic et al. in 1990<sup>[24]</sup>, the sudden reductions in density, viscosity, and thermal conductivity with increasing temperature are due to the change from a “liquid-like” to a “gas-like” supercritical state. They used a combination of theoretical predictions and the best available experimental data to develop equations for the calculation of the viscosity and the thermal conductivity.

In the review of Srinivas S. Pitla et al. they did a detailed literature research about studies on heat transfer and pressure drop in of supercritical CO<sub>2</sub> in tube flow<sup>[25]</sup>, more details can be learned.

Table 2 summarizes the figures drawn by the equations mentioned above.

**Table 2 CO<sub>2</sub> thermodynamic properties around critical point**

Property	Source	Figure
Variation of specific heat ( $c_p$ ) and the density ( $\rho$ ) of CO <sub>2</sub>	S.M. Liao, T.S. Zhao <sup>[15]</sup>	
Specific heat ( $c_p$ ) versus temperature (K) of CO <sub>2</sub>	Span. R, W. Wagner <sup>[16]</sup>	

<p>Density (<math>\rho</math>) versus temperature (K) of CO<sub>2</sub></p>	<p>Span, R, W. Wagner [16]</p>	
<p>Conductivity versus temperature (K) of CO<sub>2</sub></p>	<p>Vesovic, V, W.A. Wakeham, G.A. Olchowy, J.V. Sengers, J.T.R. Watson, J. Millat [17]</p>	
<p>Viscosity versus temperature (K) of CO<sub>2</sub></p>	<p>Vesovic, V, W.A. Wakeham, G.A. Olchowy, J.V. Sengers, J.T.R. Watson, J. Millat [17]</p>	

### 3.3 CO<sub>2</sub> transcritical cycle

The basic CO<sub>2</sub> transcritical cycle has the heat rejection process taking place in the supercritical area while the heat absorption process takes place below the subcritical area. The four main components are compressor, gas cooler, expansion valve and evaporator. According to the work from EES<sup>[26]</sup>, Fig. 1 given by Eckhard A. Groll and Jun-Hyeong Kim<sup>[27]</sup> shows the

cycle in a  $p-h$  diagram. The transcritical CO<sub>2</sub> cycles were drawn based on the following assumptions: gas cooler outlet temperature of 30 °C, evaporation temperature of 0 °C, superheat of 0 K, and isentropic compression and isenthalpic expansion processes.

It is crucial to optimize the heat rejection pressure to enhance the energy efficiency of the CO<sub>2</sub> transcritical systems. The optimum discharge pressure increases with increase in gas cooler exit temperature and decrease in evaporator temperature. Lots of theoretical studies have been done on discharge pressure optimization and various correlations have been proposed.

There are three typical approaches to develop the optimal pressure correlations: the experiments, the physics-based plant modeling and the thermodynamic cycle simulation. Table 3 shows some of the correlations in recent years.

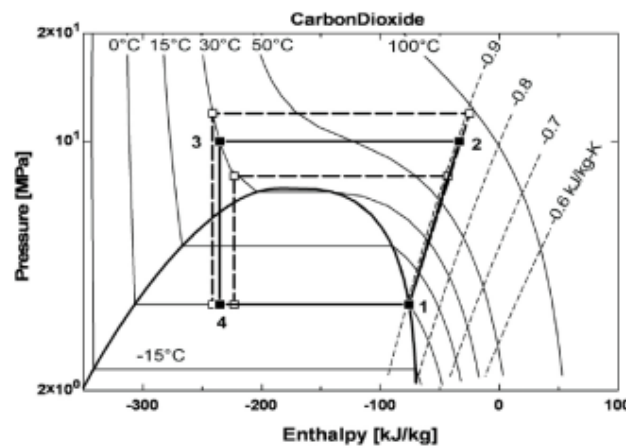


**Fig. 1 Transcritical CO<sub>2</sub> cycle in a pressure-enthalpy diagram**

**Table 3 Correlations to optimize discharge pressure**

Correlation	Year	Source	Deviation
$p_{T,H} = 2.6T_{amb} = 2.6T_c + 7.54$	1999	Friedrich Kauf	-5.8%
$p_{opt} = (2.778 - 0.0157T_e)T_c + (0.381T_e - 9.34)$	2000	S.M. Liao T.S.Zhao, A. Jakobsen	1%
$p_{opt} = 4.9 + 2.256T_{c-exit} - 0.17T_e + 0.002T_{c-exit}$	2004	J. Sarkar, S.Bhattacharyy a, M. R.Gopal	/

**Table 4 comparisons of several novel CO<sub>2</sub> transcritical cycles**

Cycle	Method	Year	Source	COP
with IHX	Modeling	2004	A. Fartaj, D. S.-K. Ting, W. W. Yang <sup>[28]</sup>	1.67
	Modeling	2005	S.G. Kim, Y.J. Kim, G. Lee, M.S. Kim <sup>[29]</sup>	3.25-3.6
IHX with vapor injection	Experiment	2012	R. Cabello, D. Sánchez, J. Patiño, R. Llopis, E. Torrella <sup>[30]</sup>	2.15-2.25
With rotary vane expander	Experiment	2011	Xiaohan Jia, Bo Zhang, Lei Pu, Bei Guo, Xueyuan Peng <sup>[31]</sup>	2-2.4
Vortex tube expansion in Maurer model	Modeling	2009	Jahar Sarkar <sup>[32]</sup>	0.86-4.96
Vortex tube expansion in Keller model				0.8-3.7
With ejector-expansion device	Modeling	2005	Daqing Li, Eckhard A. Groll <sup>[33]</sup>	2.27-2.5
With optimized ejector-expansion device	Modeling	2008	Jahar Sarkar <sup>[34]</sup>	2.1-10
With ejector-expansion device	Modeling	2011	Sun Fangtian, Ma Yitai <sup>[35]</sup>	1-4
With two ejector-expansion devices	Modeling	2012	Jiwen Cen, Pei Liu, Fangming Jiang <sup>[36]</sup>	1.7-7.2
With internal heat exchanger and ejector	Experiment	2011	Masafumi Nakagawa, Ariel R. Marasigan, Takatori Matsukawa <sup>[37]</sup>	1.1-1.8
With internal heat exchanger and ejector	Modeling	2013	Zhen-ying Zhang, Yi-tai Ma, Hong-li Wang, Min-xia Li <sup>[38]</sup>	1.5-3.5
Two stage compression split cycle	Experiment	2005	Alberto Cavallini, Luca Cecchinato, Marco Corradi, Ezio Fornasieri, Claudio Zilio <sup>[39]</sup>	1.7-3.51
Two stage compression split cycle with suction line heat exchanger				2.4-3.59
Optimized two stage compression	Modeling	2007	Neeraj Agrawal, SouvikBhattacharyya, J. Sarkar <sup>[40]</sup>	1.7-3.8
Single-throttling two stage compression	Modeling	2009	Luca Cecchinato, Manuel Chiarello, Marco Corradi, Zilio et al. <sup>[41]</sup>	0.9-3.4
Double-throttling two stage compression				2.5-3.7
Double-throttling two stage compression open flash tank				2.4-3.5

In F. Kauf's work in 1999<sup>[42]</sup>, he developed and studied how to determine the optimum high pressure by simulation and graphical method, Kauf concluded that the main influence on the optimum high pressure is the ambient temperature and the temperature of the refrigerant at the gas cooler outlet respectively. In terms of the evaporation temperature and the outlet temperature of the gas cooler, S. M. Liao et al.<sup>[43]</sup> developed the correlation for the optimal heat rejection pressure. The standard deviation between the correlation and the simulated results is less than 1%. J. Sarkar et al.<sup>[44]</sup> also did the work in transcritical CO<sub>2</sub> based simultaneous heating and cooling system with internal heat exchanger. These correlations are valid for evaporation temperatures ranging between -10 °C and 10 °C and cooler exit temperatures ranging between 30 °C and 50 °C.

There has been several ways to improve efficiency of CO<sub>2</sub> transcritical cycle. The main ways are: CO<sub>2</sub> transcritical cycle with internal heat exchanger, CO<sub>2</sub> transcritical cycle with expander, CO<sub>2</sub> transcritical cycle with vortex tube expansion, CO<sub>2</sub> transcritical cycle with ejector and CO<sub>2</sub> two-stage compression cycle. Table 4 below shows some recent research results about CO<sub>2</sub> transcritical cycle.

### **3.4 CO<sub>2</sub> heat pump**

#### **3.4.1 Air source heat pump**

Schiefloe and Nekså investigated a heat pump system for space heating combined with water heating<sup>[45]</sup> shown in Fig. 60. In order to achieve a lowest possible return temperature from the heating system, radiator and air heating are connected in series. A comparison to using R-134a as a working fluid showed favorable seasonal performance for CO<sub>2</sub> when more than 30% of the power demand for space heating were covered by the air heating system. Nekså et al. developed another novel system for space heating in 2005 taking advantage of the favorable characteristics that heat is rejected by cooling of supercritical gas at gliding temperature. By a proper design of a counter flow heat exchanger it is possible to heat air to high temperatures and thereby giving the driving force for circulation of air through the heat exchanger, in consequence without using a fan<sup>[46]</sup>. A fan-less concept, would give several advantages: no

noise, no power consumption for the fan and increased comfort with reduced air draft in the room. The concept was found to be feasible also for a high efficiency heat pump, for CO<sub>2</sub> partly characterized by a gascooler giving a low cold end approach temperature difference. It should therefore be very well suited as an indoor heat exchanger for an air-to-air heat pump for which fan noise may be an important market-limiting factor.

J. Sarkar<sup>[47]</sup> studied the steady state simulation of a transcritical CO<sub>2</sub> heat pump for simultaneous heating and cooling. The results show that optimum heat exchanger area ratio varies between 1.6 and 1.9 for maximum system COP at optimum discharge pressures.

Simulation studies on a two-stage flash intercooling transcritical carbon dioxide heat pump cycle are presented by Neeraj Agrawal and Souvik Bhattacharyy<sup>[48]</sup>. There is marginal improvement in COP as intermediate pressure decreases from the geometric mean of evaporator and gas cooler pressure. The suitability of flash intercooling two stage cycle largely depends on the refrigerant thermodynamic properties as enthalpy of evaporation is the key factor which decides the mass flow rate in the second stage compressor.

Xiao Xiao Xu et al.<sup>[49]</sup> designed adjustable ejector based on a transcritical CO<sub>2</sub> heat pump system model results. Experimental investigation showed that when the high-side pressure is increased by changing the motive nozzle area, the trend of entrainment ratio is opposite to that of pressure lift, and the ejector efficiency has a declining trend. The increased high-side pressure has a positive effect on the system performance and outweighs lower ejector efficiencies. The ejector efficiency is mainly distributed within range of 20%-30%.

### **3.4.2 Ground source heat pump**

Brian T. Austin and K. Sumathy<sup>[50]</sup> developed a numerical model has been to analyze the steady state performance of a direct-expansion geothermal heat pump using CO<sub>2</sub>. The parametric study focused on evaporator parameters including coil length, number of ground circuits and mean evaporation temperature. Performance can be further improved by optimizing the mean evaporation temperature with the surrounding soil temperature. With optimization, the system under study could achieve a COP of 2.58, representing an 18% improvement compared to the baseline system.

Young-Jae Kim and Keun-Sun Chang<sup>[51]</sup> also used simulation to do the research. The

simulation results were validated by comparing them with experimental data. The heating capacity increases by about 8.7% with the use of IHX, whereas the required compression power increases by about 10.6% due to the increase of the compressor outlet pressure resulted from the reduction of EEV opening.

### **3.4.3 Heat pump water heater**

Petter Nekså et al. did a detailed introduction on CO<sub>2</sub> heat pump water heater in 1998<sup>[52]</sup>, introduced the theory and prototype design. The prototype was designed and constructed in a NTNU-SINTEF laboratory, The calculations were carried out for an Oslo climate, using air as heat source. This means that with this system, the energy consumption for tap water heating can be reduced by 75%, compared with direct heating with electricity. Another big advantage for the CO<sub>2</sub> HPWH-system is that it can produce hot water at temperatures up to 90 °C without any operational problems.

## **3.5 Different kinds of solar assisted heat pump systems**

The basic solar system is a standard liquid heating system. It consists of conventional heating collectors, and an anti-freeze collector loop, a heat exchanger between the collector and storage, a storage tank, a liquid-to-air heat exchanger coil in the house supply duct, auxiliary space and water heaters, and a common control strategy. The basic heat pump system includes a conventional three-ton-air-to-air heat pump which has a coil in an outdoor unit and a coil indoor to supply the house need<sup>[53]</sup>.

G.Panaras et al.<sup>[54]</sup> investigated the performance of a combined solar thermal heat pump hot water system. They use a heat pump as an auxiliary energy source for solar domestic hot water systems to achieve significant energy savings, due to the remarkable potential of heat pumps on the efficient provision of thermal energy. The performance of the system on an annual basis is investigated according to the climatic data of Athens. The temperature set-point for the activation of the heat pump proves to be an important parameter for the performance of the system, noting that the higher the value of the set-point, the lower the efficiency of the heat pump.



S. Deng et al.<sup>[55]</sup> used carbon dioxide heat pump, which has proven to be a good method for supplying heating and DHW for residential buildings. Due to the difficulty that CO<sub>2</sub> heat pump has for meeting year round demands of a residential building only using CO<sub>2</sub> heat pump because of its unsatisfactory cooling efficiency. The energy consumption of the novel CO<sub>2</sub> heat pump is compared with that of a conventional CO<sub>2</sub> heat pump in one case study. This hybrid heat pump integrates a small scale solar thermal driven absorption chiller (ABS) and a CO<sub>2</sub> heat pump. This system also has a novel swing compressor has been employed in the CO<sub>2</sub> heat pump loop to match the CO<sub>2</sub> characteristics<sup>[56]</sup>. After the gas cooler of the CO<sub>2</sub> heat pump, the evaporator of the ABS chiller comes into the loop in addition. This structure aim at lowering down the temperature of CO<sub>2</sub> working fluid when it leaves the gas cooler, thus the temperature difference of super-cooling is increased, which has good effect on raising the efficiency of CO<sub>2</sub> heat pump.

O.Ozgener and A.Hepbasli<sup>[57]</sup> emphasized the advantages that ground source heat pump has over air source heat pumps. The ground source heat pumps consumes less energy to operate and uses less refrigerant. It has a simpler design and consequently less maintenance and does not require the unit to be located where it is exposed to weathering. Though the ground source heat pump has higher initial cost, being about 30-50% more expensive than air source units, but the savings due to the COP, the payback time is acceptable.

A lot of researchers shared the same interests. In Canada, F.M.Rad, A.S.Fung and W.H.Leong<sup>[58]</sup> examined the viability of hybrid ground source heat pump systems that use solar thermal collectors as the supplemental component in heating dominated buildings. The study showed that the solar thermal energy storage in the ground could reduce a large amount of ground heat exchanger length. The solar thermal collector was used as above-ground heat exchanger. An actual residential building was modeled and result was compared to the actual data that were collected by monitoring the related operation of equipment through some specific months. After the house model and SAGSHP model were conducted, more detailed analysis such as sensitivity of the ground thermal conductivity, solar collector area and ground loop heat exchanger length relation and system cost was looked into.

E.Wang et al.<sup>[59]</sup> presented a novel hybrid solar ground source heat pump system which consists of a ground source heat pump and a solar assisted ground source heat pump in an office

building for heating and cooling. Using the ground source heat pump, there is something should be taken into consideration. As the ground is usually used as the heat or cool source during the heating or cooling season to meet the load requirement of the building, the amount of heat injected to or drawn from the ground should reach some balance during every year's operation to make sure the ground temperature and other characteristics stay the same in the long term. If the annual temperature fails to remain the same, this could result in function failure of ground source heat pumps. Wang mainly focused on the severely cold places, where heating requirement is much higher than cooling requirement, and used solar energy as auxiliary energy source used in such regions.

In sum, solar assisted heat pump systems, are recognized to be outstanding heating, cooling and water heating systems. But there is still few investigation about solar assisted ground source heat pump system using CO<sub>2</sub> as refrigerant. The investigations listed above can be really good reference for the further study of this new system, and offer good example for simulation. It may be concluded that with suitable technology and investigation, there are a lot more improvements can be made from the basic solar assisted heat pump system, thus they may be playing a leading role in the modern, sustainable environment.

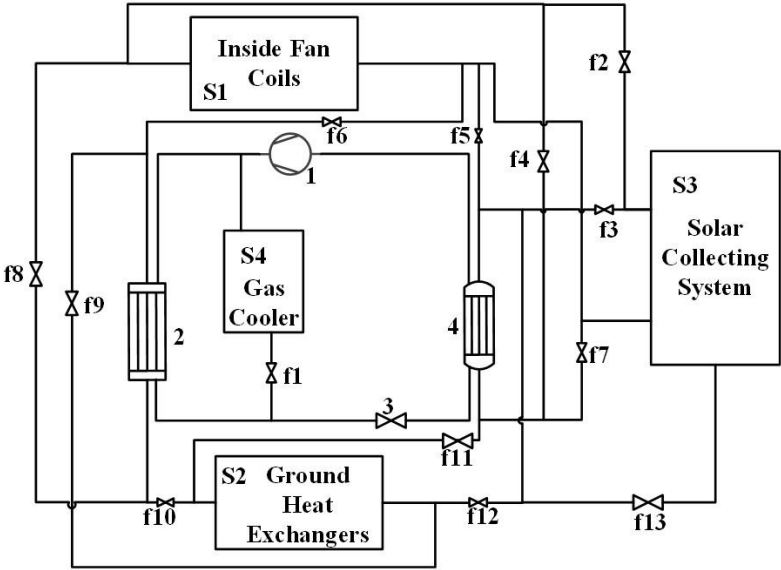
## 4 System design and key performance indexes

### 4.1 System design

The main idea of the proposed system is to reduce the unbalance of soil heat on annual basis for cold-climate areas by solar collector and for hot climate areas by CO<sub>2</sub> gas cooler. The solar energy is used to provide auxiliary heat when the ground heat is used as the heat source, to reduce the difference between the heat extracted from and rejected to the soil. Meanwhile the gas cooler is used to release excess heat to the air rather than to the soil. Fig. 2 is the overview of the system. Fig. 3 illustrates the system in areas with more cooling demands than heating demands and Fig. 4 illustrates the system facing heating dominant areas.

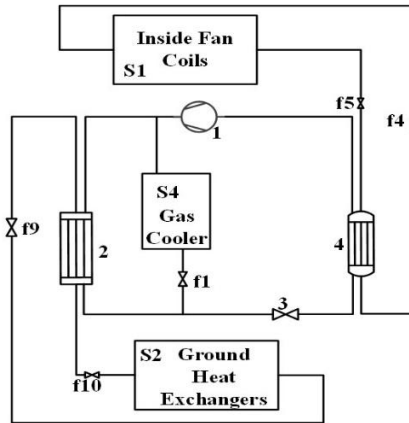
It can be seen in Fig. 2 that the system contains a complete ground source heat pump, which consists of a heat pump (consisting components 1, 2, 3 and 4) and a series of underground heat exchangers. The solar assisted function is realized by a solar energy collecting system, shown as S3 in Fig. 1, which contains a solar collector, a solar pump, and a water tank. The ground source heat exchanger is combined with the heat pump system, connected to the heat exchanger 2 or 4, depending on the operating mode of the system. The solar energy collecting system is combined with the heat pump by connecting to the exchanger 4 as well as with the building by connecting to the inside fan coils system shown as S1 in Fig. 1. The gas cooler is referred to as S4 in Fig. 2. In this system, the working fluid is circulating in the heat pump system, and water is working as media in the proposed system to transfer heat from the ground source system or solar collecting system to the heat pump system. There are all together 13 valves shown in the system schematic diagram, annotated from f1 to f13. The valves control the circulation of the fluid and help change the operating mode of the system. In cooling mode, valves f4, f5, f9 and f10 are open, ground heat exchanger S2 connects with condenser 2. In heating mode, f1, f4, f5, f9 and f10 stay closed. Ground heat exchanger connects with evaporator 4 by valves f3 and f7. When it is needed to charge the solar collected heat into the soil, f13 is open so the heated water could go through ground heat exchanger to

exchange heat with earth.



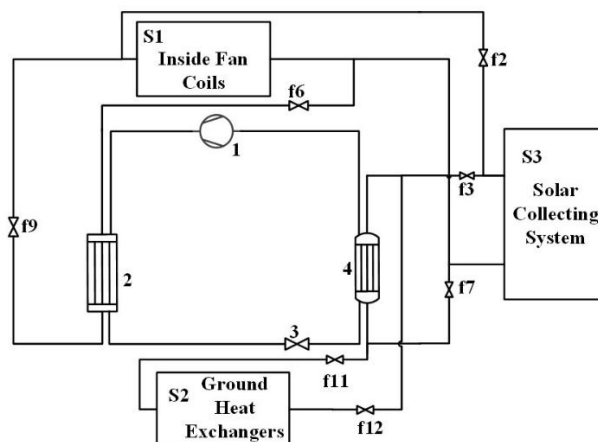
**Fig. 2 Whole system schematic diagram**

Fig. 3 shows the system’s cooling mode when working in areas where the cooling demand is much higher than heating demand, thus too much heat is rejected to the soil and soil temperature will increase on annual basis. Normally valves f4, f5, f9 and f10 stay open and f1 opens when the cooling load keeps going up to some level. Heat exchanger 4 works as the evaporator of the heat pump and is connected with the inside fan coils to provide the cooling capacity for the building, and the heat exchanger 2 works as condenser and is connected with the ground heat exchanger and gas cooler. The supercritical refrigerant from compressor enters into the gas cooler, where the working fluid is cooled by air and also by the water circulated in the ground heat exchanger. When the cooling load reaches to certain number, which is decided according to the specific unbalance situation in various cities, f1 opens and some of the supercritical working fluid from compressor enters into the gas cooler, and some exchange heat with the water circulating in the ground heat exchanger. Therefore, the cooling capacity of gas cooler can be divided between by air and water.



**Fig. 3 System schematic diagram in cooling mode in hot summer area**

Fig. 4 is the schematic diagram of how the system operates in winter in areas where heating demand is much higher than cooling demand, thus more of the heat is extracted from the soil than that is rejected into the soil, the soil temperature will decrease on annual basis. There are alternative ways to use when combine solar energy to the ground source heat pump, to make the most use of the energy and improve the performance of the new hybrid system, the main control modes of the system are: (1) Using water tank as another source of heat as well as the soil in heating season, open valves f3, f6, f7, f8, f11 and f12, the inside fan coils S1 connects with condenser 2; (2) When water temperature at the outlet of the storage is higher than the needed temperature for space heating (35 °C for a floor heating terminal and 45 °C for a fan coil heating terminal), open valves f2, f6, f8, f11, f12 and f16, the heat collected by the water tank goes directly to the building to heat the room while the ground heat exchangers S2 still connected to the evaporator acting as the heat source.



**Fig. 4 System schematic diagram in heating mode in cold winter area**

Fig. 5 shows the charging mode in heating dominant areas in summer. Since the amount of heat extracted from the soil is much more than that injected to the soil in these area, gas cooler in summer is not necessary. In this mode, the collected heat by solar collectors is given to the soil by the ground heat exchangers. The connecting valves f12 and f13 are open. Those area has less quantity of heat in summer, so not all the underground heat exchangers are essential. Part of the heat exchangers are used to give the heat back to soil, in which case compensates the heat taken from the soil in winter in another way.

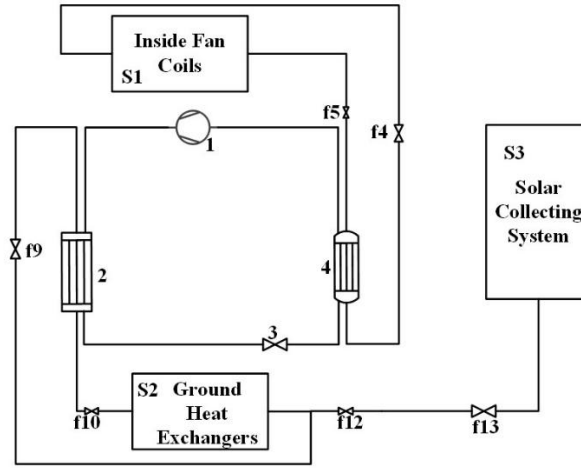


Fig. 5 System schematic diagram in charging mode in cold winter area

## 4.2 Key performance indexes

The cooling and heating capacities for the building are calculated by Eqs. (3) and (4), respectively.

$$Cap_{cooling} = m_{w,e} Cp_w (T_{o,e} - T_{i,e}) \quad (3)$$

$$Cap_{heating} = m_{w,c} Cp_w (T_{o,GC} - T_{i,GC}) \quad (4)$$

The heat exchanged between the soil and the heat pump system is defined by Eqs. (5) and (6) respectively.

$$Q_{absorb,heating} = Cap_{heating} - P_{heating} \quad (5)$$

$$Q_{reject,cooling} = Cap_{cooling} + P_{cooling} \quad (6)$$

Air cooling load proportion is defined as the ratio of the cooling capacity of air-cooled gas cooler to the total cooling capacity of air-cooled and water-cooled gas coolers in the system:

$$\varphi_{Air,cooling} = \frac{Q_{cooling,GC}}{Q_{cooling,tot}} \quad (7)$$

The earth's energy imbalance degree is defined as:

$$\Delta E_{un} = \frac{|Q_{cooling} - Q_{heating}|}{\max(Q_{cooling}, Q_{heating})} \times 100\% \quad (8)$$

The coefficient of performance of the system of heating and cooling mode is expressed respectively as:

$$COP_{heating} = \frac{Cap_{heating}}{P_{heating}} \quad (9)$$

$$COP_{cooling} = \frac{Cap_{cooling}}{P_{cooling}} \quad (10)$$

## 5 Mathematical modeling of the system

### 5.1 Heat pump model

For the compressor, the power depends on the R744 mass flow rate, the total efficiency and the isentropic change in R744 enthalpy:

$$\dot{W}_{\text{comp}}^{\text{g}} = \frac{\dot{m}_c (h_{2,\text{isen}}^{\text{g}} - h_1^{\text{g}})}{\eta_{\text{tot}}} \quad (11)$$

$$\dot{m}^{\text{g}} = V_s \cdot \eta_{\text{vol}} \cdot N \cdot \rho_1 \quad (12)$$

where,  $V_s$  is the swept volume,  $N$  is the compressor speed and  $\rho_1$  is the suction density;  $\eta_{\text{tot}}$  and  $\eta_{\text{vol}}$  are compressor's total efficiency and volumetric efficiency, respectively, which is assumed to correspond with Ortiz et al. correlation<sup>[60]</sup> for R744, shown as below.

$$\eta_{\text{tot}} = -0.26 + 0.7952 \left( \frac{P_2}{P_1} \right) - 0.2803 \left( \frac{P_2}{P_1} \right)^2 + 0.0414 \left( \frac{P_2}{P_1} \right)^3 - 0.0022 \left( \frac{P_2}{P_1} \right)^4 \quad (13)$$

$$\eta_{\text{vol}} = 0.9207 - 0.0756 \left( \frac{P_2}{P_1} \right) + 0.0018 \left( \frac{P_2}{P_1} \right)^2 \quad (14)$$

For the gas cooler, as in Fig. 6 shows, under the cooling mode, the gas cooler is cooled by the ambient air and water coming from ground heat exchanger in series; while under the heating mode, the gas cooler is cooled by water coming from fan coils of AHU. Pressure drop of R744 through the gas cooler is evaluated using a Darcy friction factor calculated by Blasius correlation<sup>[61]</sup>.

For the water-cooled gas cooler, it is a counter-flow, concentric tube heat exchanger with R744 flowing in the inner-tube and water flowing through the annular tube. Figure 6 represents one element of the water-cooled gas cooler. Properties are assumed to be constant throughout the control volume element. Outlet conditions for one element are calculated, and these become the inlet conditions for the next element. The overall gas cooler analysis is then carried out by successively calculating the pressure drop, temperature change and heat transfer rate in each element. For each control volume segment shown in Fig. 6, energy



gained by water must equal to the energy rejected by R744<sup>[62]</sup>. Thus energy balance equations can be equated as follows:

$$\dot{Q}^i = \dot{m}_w c_{p,w} (T_w^i - T_w^{i+1}) = \dot{m}_w c_{p,c} (T_c^i - T_c^{i+1}) \quad (15)$$

$$\dot{Q}^i = \varepsilon C \min(T_c^i - T_w^{i+1}) \quad (16)$$

$$\varepsilon = \frac{1 - \exp[-NTU(1-R)]}{1 - C \times \exp[-NTU(1-R)]}, NTU = \frac{UA}{C \min}, R = \frac{C \min}{C \max} \quad (17)$$

In Eq. (17), the overall heat transfer coefficient ( $UA$ ) is obtained as the sum of the resistivity values, including convective resistance of R744, conductive resistance of tube-wall and convective resistance of water. The water inlet temperature is the same as the outlet water temperature of ground heat exchanger, which is calculated by Eq. (21).

For the expansion valve, the model is denoted as:

$$h_{in} = h_{out} \quad (18)$$

For the evaporator, the thermal equilibrium equation is expressed as:

$$\dot{m}_w C p_w (T_{in} - T_{out}) = \dot{m}_r (h_{1,r} - h_{4,r}) \quad (19)$$

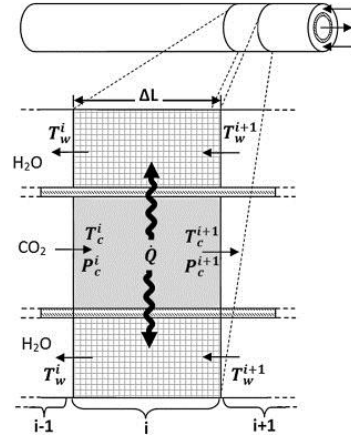


**Fig. 6 Single control volume segment of gas cooler**

## 5.2 Underground heat exchanger model

The temperature distribution of the soil around the U-tube is calculated by the following equation:

$$\frac{\partial T_g}{\partial \tau} = \alpha_g \left( \frac{\partial^2 T_g}{\partial x^2} + \frac{1}{x} \frac{\partial T_g}{\partial x} \right) \quad (20)$$

where,  $T_g$  is soil temperature,  $\alpha_g$  is thermal diffusivity of soil,  $\tau$  is time,  $x$  is the distance to the borehole center.

The heat transfer between ground heat exchanger and soil is calculated by:

$$Q_{GX} = m_{w,GX} C_{p,w,GX} |T_{in,GX} - T_{out,GX}| \quad (21)$$

The temperature distributions of the water in the inlet and outlet U-tubes are given by Eqs. (14) and (15), respectively<sup>[63],[64],[65]</sup>:

$$\theta(Z) = \cos h(\beta Z) - \frac{1}{\sqrt{1-P^2}} \times \left[ 1-P \frac{\cos h(\beta) - \sqrt{\frac{1-P}{1+P}} \sin h(\beta Z)}{\cos h(\beta) + \sqrt{\frac{1-P}{1+P}} \sin h(\beta Z)} \right] \sin h(\beta Z) \quad (22)$$

$$\theta(Z) = \frac{\cos h(\beta) - \sqrt{\frac{1-P}{1+P}} \sin h(\beta)}{\cos h(\beta) + \sqrt{\frac{1-P}{1+P}} \sin h(\beta)} \cos h(\beta Z) + \frac{1}{\sqrt{1-P^2}} \times \left[ P \frac{\cos h(\beta) - \sqrt{\frac{1-P}{1+P}} \sin h(\beta Z)}{\cos h(\beta) + \sqrt{\frac{1-P}{1+P}} \sin h(\beta Z)} - P \right] \sin h(\beta Z) \quad (23)$$

$$\beta = \frac{H}{m_W C_{p_W} \sqrt{(R_{11}+R_{12})(R_{11}-R_{12})}} \quad (24)$$

where,  $\theta$ ,  $Z$  and  $P$  are nondimensional temperature, length and thermal resistanc, respectively;  $m_W$  and  $C_{p_W}$  are mass flow rate and specific heat of water inside tube, respectively.

Detailed parameter of ground source heat exchanger used in this thesis is given by Table 5.

**Table 5 Ground source heat exchanger parameter**

Parameter	Number
Distance between boreholes /m	4
Depth of the boreholes /m	80
Diameter of the boreholes /mm	160
U-tube material	PE
U-tube type	DN32
U-tube conductivity /W(m <sup>-1</sup> K <sup>-1</sup> )	0.46
Shank spacing between the tubes /mm	80
Soil type	Sand clay
Soil conductivity /W(m <sup>-1</sup> K <sup>-1</sup> )	1.86

### 5.3 Solar collector model

For solar collector, a theoretical flat-plate collector model is chosen. This component models the thermal performance of a theoretical flat plate collector. The total collector array may consist of collectors connected in series and in parallel. The thermal performance of the total collector array is determined by the number of modules in series and the characteristics of each module. This model provides for the theoretical analyses of a flat plate. The Hottel-Whillier steady-state model is used for evaluating the thermal performance.

The energy collection of each module in an array of  $N_s$  modules in series is modeled according to the Hottel-Whillier equation such that ( $j$  is the module number):

$$Q_{useful} = \frac{A}{N_s} \sum_{j=1}^{N_s} F_{R,j} \left( I_T(\tau\alpha) - U_{L,j}(T_{i,j} - T_a) \right) \quad (25)$$

Where

$$F_{R,j} = \frac{N_s \dot{m}_c C_{pc}}{AU_{L,j}} \left( 1 - \exp \left( - \frac{F' U_{L,j} A}{N_s \dot{m}_c C_{pc}} \right) \right) \quad (26)$$

### 5.4 Water storage tank model

A stratified fluid storage tank is chosen. The thermal performance of a fluid-filled sensible energy storage tank, subject to thermal stratification, can be modeled by assuming that the tank consists of  $N$  ( $N \leq 15$ ) fully-mixed equal volume segments. The degree of stratification is determined by the value of  $N$ . If  $N$  is equal to 1, the storage tank is modeled as a fully-mixed tank and no stratification effects are possible. Options of fixed or variable inlets, unequal size nodes, temperature deadband on heater thermostats, incremental loss coefficients, and losses to gas flue of auxiliary heater are all available.

The tank has 3 modes itself. In mode 1, flow streams enter the tank at fixed positions. The load flow enters at the bottom of the tank and the hot source stream enters just below the auxiliary, if present, or at the top of the tank if no auxiliary is specified. At the end of each time interval, any temperature inversions that exist are eliminated by total mixing of the appropriate adjacent nodes. In mode 2, the flowstream enters the node that is closest to it in temperature. With sufficient nodes, this permits a maximum degree of stratification. In mode

3, the user must specify the nodes containing the load flow and source flow inlet locations.

The temperatures of each of the N tank segments are determined by the integration of their time derivatives. At the end of each timestep, temperature inversions are eliminated by mixing appropriate adjacent nodes.

The temperature of each of the N tank segments are determined by the integration of their time derivatives. At the end of each time step, temperature inversions are eliminated by mixing appropriate adjacent nodes.

Energy flows and change in internal energy are calculated as follows:

$$Q_{env} = \sum_{i=1}^N UA_i (T_i - T_{env}) + \gamma_f \sum_{i=1}^{i=l} (UA)_{f,i} (T_i - T_f) \quad (27)$$

$$Q_s = m_L C_{pf} (T_1 - T_L) \quad (28)$$

$$Q_{in} = m_h C_{pf} (T_h - T_N) \quad (29)$$

Where  $Q_s$  is the rate at which sensible energy is removed from the tank to supply the load,  $Q_{in}$  is the rate of energy input to tank from hot fluid stream,  $m_L$  is the fluid mass flow rate to the load and/or of the makeup fluid,  $m_h$  is the fluid mass flow rate to tank from the heat source,  $C_{pf}$  is specific heat of the tank fluid,  $T_N$  is the temperature of fully mixed fluid of layer N,  $T_L$  is temperature of the fluid replacing that extracted to supply the load,  $T_h$  is temperature of the fluid entering the storage tank from the heat source.

## 5.5 Air cooled gas cooler

For the air-cooled gas cooler, the performances can be predicted by the generalized heat transfer and frictional correlation proposed by Wang et al.<sup>[66]</sup>, which will be verified by the experimental data of ambient air cooled-gas cooler in Section 6.

## 6. Model validation

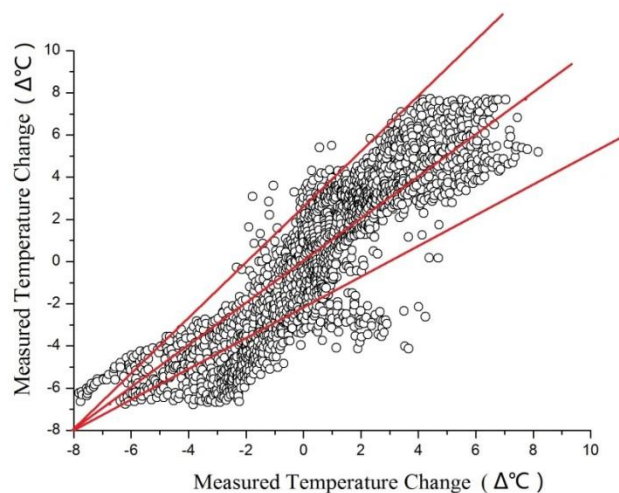
### 6.1 Heat pump model validation

Scott Hackel and Amanda Pertzborn<sup>[67]</sup> validated the heat pump model that is used in this

thesis. Initially validation of the GHX model was completed for all four fields at Cashman individually; the mean bias error (MBE) of the model for calculating  $\Delta T$  across those four fields was  $2\text{ }^{\circ}\text{C}$  [68].

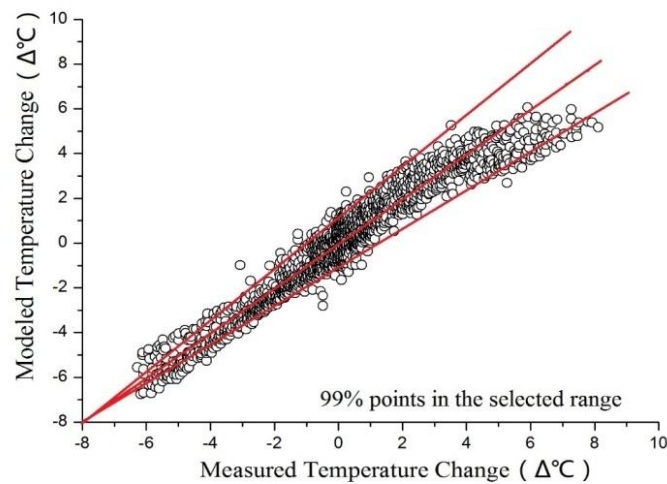
They validated the whole system model with their experimental data. Measurements of temperature and flow rate were acquired from a cooling tower GSHP system near Las Vegas, Nevada (Site 1), and from a system in Madison, Wisconsin (Site 2). At Site 1, the measurements are acquired instantaneously at 15-min intervals; at Madison, Wisconsin, the measurements are acquired continuously with a sample rate of 1 Hz and averaged over each 15-min time period. The modeled and measured data matched very closely and error (in  $T_{fl,in}$ ) was only  $1\text{ }^{\circ}\text{C}$  ( $1\text{--}2\text{ }^{\circ}\text{F}$ ) at peak load conditions.

Fig. 7 shows the comparison of results from modeling and experimenting.  $\Delta T$  is defined as the fluid temperature at inlet to field minus the fluid temperature at the outlet of field. The line indicates where the modeled results match the measured results perfectly. Even though some data is not quite agree with each other, a considerable amount of data points lay around the line, showing good predictive ability of the model.



**Fig. 7 Measured and modeled results of temperature change**

When using the data points corresponding to full flow, the results coming out of Fig. 7 shows better match as in Fig. 8. These data points are selected based on the criteria that the flow is greater than  $60\text{ m}^3/\text{hr}$  ( $264\text{ gpm}$ ), and the assumption that this is the flow for the full time step.

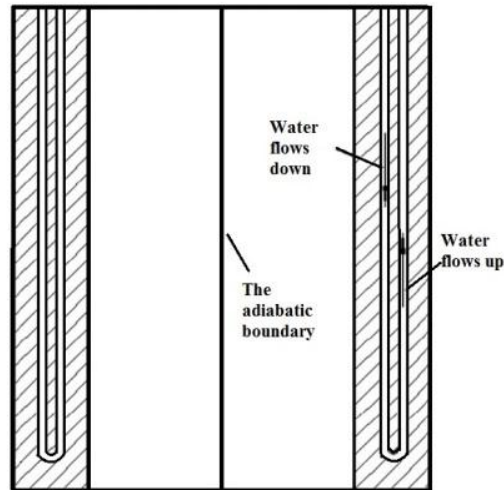


**Fig. 8 Measured and modeled results of temperature change without low flow data**

## **6.2 Underground heat exchanger model validation**

Fig. 9 shows the theoretical model of the underground heat exchanger. X. Q. Zhai<sup>[69]</sup> used the model to simulate and compared the simulated results to his experimental results. There are several assumption rules when using this model to simulate:

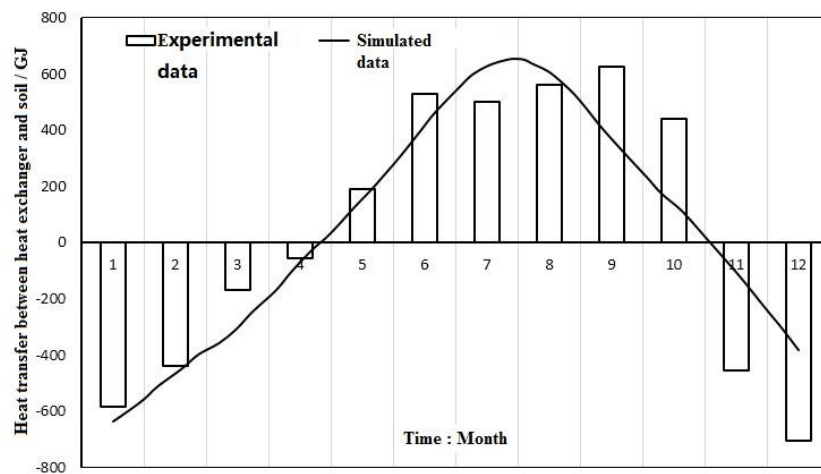
- (1) The ground soil is homogeneous;
- (2) The thermal properties of all the materials remain constant within the temperature range investigated;
- (3) There is no contact resistance between the boreholes and the ground;
- (4) The ground temperatures at the top surface and far below the boreholes remain constant;
- (5) For the short time analysis, the axial temperature variation is ignored.



**Fig. 9 Schematic diagram of theoretical model**

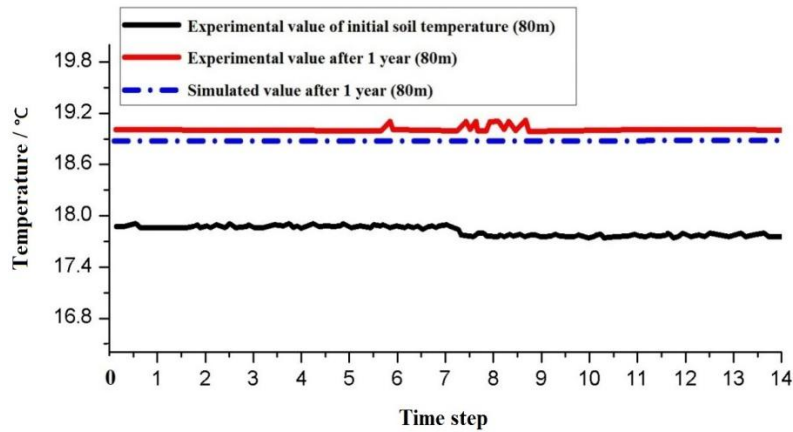
The experimental object was Shanghai Minhang archive, the is  $8000\text{m}^2$ . There were at all 280 boreholes, the depth of the borehole was 80m and the diameter of the borehole was 160mm. According to the experimental data, Fig. 10 compared the tested amount of heat exchanged between heat exchanger and the soil with modeled results. Fig. 11 shows the results of soil temperature change from experimental data and simulated results respectively.

Fig. 10 shows the simulated heat transfer results between underground heat exchanger and soil agree quite well with the experimental data. Even though the experimental data is gained month by month and simulated results are gained continuously, the line of simulated results appears to have the same variation tendency with the experimental data. Besides, the peak of each month is approximately the same.



**Fig. 10 Experimental and modeled data of heat transfer between heat exchanger and soil**

Fig. 11 indicates the soil temperature change from measured data and modeled results. After a year of operation, the simulated value of soil temperature and experimental value of soil temperature is almost the same at depth 80m. This result and results from Fig. 10 shows the model of underground heat exchanger has good predictive ability and high reliability.



**Fig. 11 Experimental and simulated value of soil temperatures**

### 6.3 Solar collector and water storage tank model validation

In the paper Carsen J. Banister et al.<sup>[70]</sup> used the same solar collector model and hot water storage tank model as in this thesis and validated the models in Ottawa, Canada by experimental results.

The validation process comprises of running both the experimental apparatus and the model for a particular day, recording the relevant measurements such as temperature and energy transfer, and comparing the results. Since temperature is a good indication of how much energy transfer has taken place, this is the main method of comparison used. The volume and substance within the system are constant, meaning that changes in temperature are directly proportional to the amount of energy exchanged.

Two representative days, August 14 and October 29, were chosen to validate the model developed. The former day is typical summer weather, whereas the latter is typical fall weather. Results of day 1, August 14 and day 2, October 29 are shown in Fig. 12 and Fig. 13 respectively.



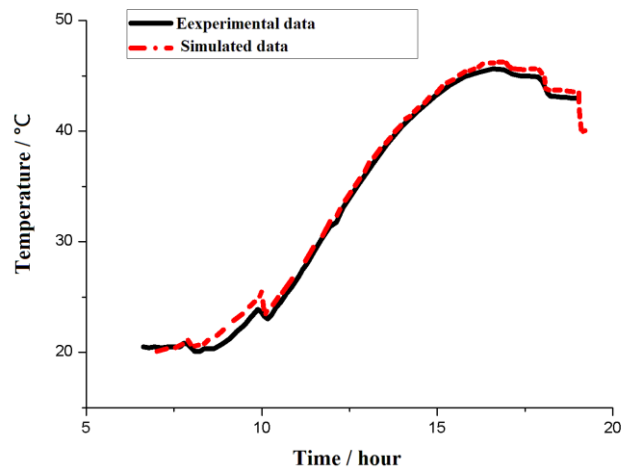


**Fig. 12 Tank average temperature comparison, day 1**

Day 1 is one of the particular days with clear skies and very high amounts of solar irradiation. The horizontal irradiation peaks around 3600 (kJ/h m<sup>2</sup>), supplying large amount of solar energy to the system.

The results in Fig.12 shows the tank temperature starts around room temperature at 20 °C and is heated to just over 45 °C by the end of the day. Although the tank will typically not experience temperatures as low as 20 °C, these initial conditions were selected to ensure that the system ran for as much time as possible. In addition, it was also important to validate the model at lower than typical temperatures.

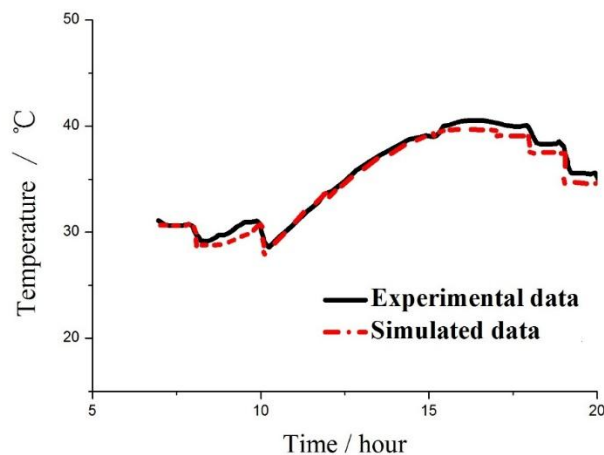


**Fig. 13 Tank average temperature comparison, day 2**

The second test day, October 29, represents a fall day where the solar irradiation is not as high as the summer day and experiences more variation due to cloud cover.

As in Fig. 13 shows, energy collection during this day was less than that for the summer day, as would be expected. For this case the tank temperatures began around 30 °C and were only able to reach about 40 °C at the peak. In both cases, the sharp drops seen in tank temperature is due to water being drawn through the system. The rising temperatures are due to heat being added to the tank via the heat pump and solar thermal collector.

#### 6.4 Air cooled gas cooler model validation

In the present study, the model of the ambient air-cooled gas cooler was validated by the experimental data, covering the operation conditions of the ambient temperatures from 25 °C to 45 °C and the inlet pressures of R744 in gas cooler from 75 Bar to 120 Bar, as shown in Table 6. The model deviations are within 10%, meaning that the model's accuracy is sufficient for the investigation of the proposed system.

**Table 6 Experimental data of air cooled gas cooler**

<b>Ambient Temp. °C</b>	<b>Inlet Pressure Bar</b>	<b>Inlet Temp. °C</b>	<b>Outlet Temp. °C</b>	<b>Load Energy KW</b>	<b>Mass Flow of R744 kg/h</b>	<b>Pressure Drop of R744 Bar</b>
25	75	88	27	171	2641.54	0.03
25	75	88	25.4	171	2565.98	0.028
30	78.5	88	32	342	6064.27	0.12
30	78.5	88	30.4	342	5704.51	0.11
35	92	88	37	570	11184.38	0.3
45	85	88	47	395	30857.14	2.37
45	120	88	47	240	11074.29	0.5
45	120	140	45.4	335	18120	0.28

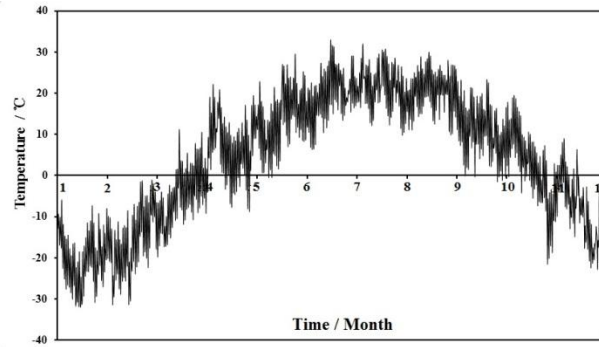
## **7. Performance simulation and economic analysis**

The whole system is assembled and the abovementioned mathematical models are finally connected to the environmental module to simulate its performance under the chosen city's TMY (typical meteorological year) data. Temperatures, wind speeds and solar radiations at regular time intervals are read in by a data processor to generate direct and diffuse radiation outputs for a number of surfaces with arbitrary orientation and inclination.

### **7.1 Weather data and operation schedule**

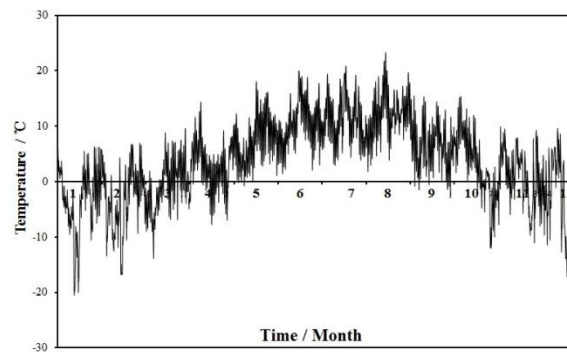
The system was run in four typical cities. Harbin, China and Trondheim, Norway were chosen as typical cold winter climate city to test the solar assisting function of the system since this two city has long and cold winter but their summer days are not quite long and not quite hot, either. Shanghai, China and Guangzhou, China were chosen as typical hot summer climate city to test the air cooled gas cooler function for the system since this two city has rather long and hot summer but their winter days are not quite long and not quite hot, either. In Shanghai, the ambient temperature of winter can reach as low as  $0^{\circ}\text{C}$  and in Guangzhou, most of the days in winter has temperature around  $10^{\circ}\text{C}$ .

Fig. 14 shows the hourly ambient temperature of Harbin month by month. From the data from Fig. 14, it can be seen that summer highest temperature can barely reach  $30^{\circ}\text{C}$  for most of the days, but in winter the temperature easily goes down to  $-10^{\circ}\text{C}$  and sometimes reaches  $-30^{\circ}\text{C}$ .



**Fig. 14 Ambient temperature of Harbin (2010)**

Fig. 15 shows the hourly ambient temperature of Trondheim month by month. From the data from Fig. 15, it can be seen that summer ambient temperature in Trondheim is quite moderate in this chosen year. The days when temperature reaches higher than 20° C is not a lot and most of the days temperature stays between 10° C to 20° C. meanwhile, winter temperature can reach as low as -20° C and most of the time stays around -5° C.



**Fig. 15 Ambient temperature of Trondheim (2008)**

Thus the operation schedule of Harbin, Trondheim, Shanghai and Guangzhou can be seen in Table 7. Since the designed parameter for indoor is: temperature-20 °C and humidity-50% for winter; temperature-25 °C and humidity-60% for summer, the periods of cooling, heating and transition seasons were determined accordingly. For Harbin, winter season is the whole months of January, February, March, April, September, October, November and December.

According to the temperature data, the operation schedule of Trondheim can be seen in Table 7. Since the temperature and humidity is moderate in some season, it is chosen in part of May and part of September to be transition season where neither heating or cooling is needed.

**Table 7 Operation schedule of different cities**

City	Winter	Summer	Transition
Harbin	0-2880h, 5833-8760h	2881-5832h	/
Trondheim	0-3320h, 5936-8760h	3625-5832h	3321-3624h, 5833-5935h
Shanghai	0-2880h, 7291-8760h	2881-7290h	/
Guangzhou	0-2160h, 8017-8760h	2161-8016h	/

In the same way, the operation schedule of Shanghai and Guangzhou is decided as shown in Table 9. Due to its high ambient temperature, Guangzhou needs cooling in most of the year, but it needs heating only in January, February and December.

## 7.2 Simulation and analysis for solo R744 GSHP

To compare the novel systems with solo R744 ground source heat pump system, one base case model was built using the validated heat pump system model and the validated ground source heat exchanger model. To connect all the components, TRNSYS 6.1 was used to run the simulation. The base case is calculated on the conventional ground source heat pump system, the simplified system schematic is illustrated in Fig. 16.

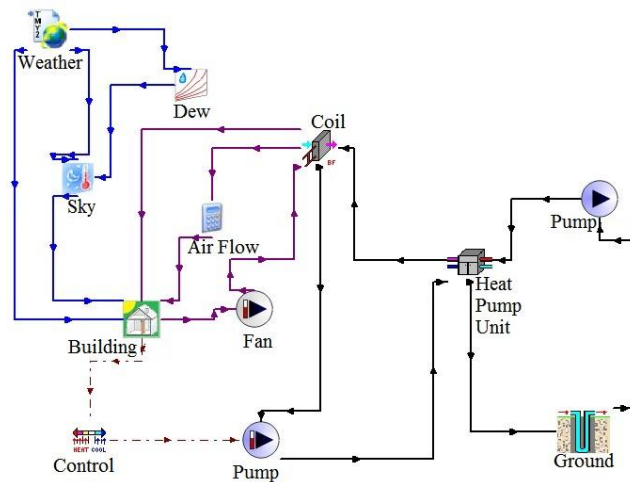


**Fig. 16 Simplified system schematic of solo R744 GSHP**

As about the building model, we simulated an 8000m<sup>2</sup> area office building, it consists of four floors, each floor has the construction area of 2000m<sup>2</sup>. The construction style of the building can be modified, in Chinese style building, the structure is basically concrete style and in Norwegian style building, the structure is light wooden style.

**Table 8 Energy loads of solo GSHP system in Harbin**

Month	Harbin	
	Cooling load/GJ	Heating load/GJ
1	—	209.45
2	—	184.72
3	—	199.87
4	—	144.36
5	99.49	—
6	166.10	—
7	126.59	—
8	125.05	—
9	—	71.91
10	—	165.39
11	—	183.35
12	—	185.91
Whole year	517.23	1344.96
Unbalance	61.6%	

Table 8 shows the monthly energy loads when using a solo CO<sub>2</sub> ground source heat pump as the air conditioning supply in Harbin. From the table data it is easy to come to the conclusion that the heating operation time is much longer than the cooling operation time, and since the temperature is not very high in summer yet rather low in winter, the cooling load is much lower than the heating load on annual basis. At the bottom of the Table.1 one the annual imbalance of the ground heat load is calculated and the result is 61.6%, which is very high.

Table 9 shows the monthly energy loads when using a solo CO<sub>2</sub> ground source heat pump in Trondheim. For Trondheim, two different kinds of building structure were used. One is Chinese concrete structure used before and the other is typical Norwegian building structure in 1980s, which is light wooden structure. Ceilings, floor and windows are 200mm thick and out wall is 150mm thick.

**Table 9 Energy loads of solo GSHP system in Trondheim**

Month	Norwegian structure		Chinese structure	
	Cooling load/GJ	Heating load/GJ	Cooling load/GJ	Heating load/GJ
1	—	157.07	—	156.64
2	—	139.66	—	139.66
3	—	151.96	—	151.96
4	—	144.43	—	141.88
5	—	87.045	—	82.79
6	16.69	—	26.93	—
7	21.91	—	36.67	—
8	19.85	—	26.55	—
9	—	114.44	—	110.92
10	—	136.21	—	138.67
11	—	130.06	—	134.18
12	—	132.67	—	136.67
Whole year	58.45	1193.57	90.16	1193.40
Unbalance		95.1%		92.4%

**Table 10 Energy loads of solo GSHP system in Shanghai**

Month	Shanghai	
	Cooling load/GJ	Heating load/GJ
1	—	568.06
2	—	480.17
3	—	428.10
4	—	169.65
5	263.66	—
6	568.18	—
7	966.03	—
8	944.32	—
9	554.00	—
10	149.29	—
11	—	282.56
12	—	502.05
Whole year	3445.48	2430.58
Unbalance		29.5%

**Table 11 Energy loads of solo GSHP system in Guangzhou**

Month	Guangzhou	
	Cooling load/GJ	Heating load/GJ
1	—	174.93
2	—	164.70
3	—	91.69
4	348.39	—
5	692.64	—
6	826.14	—
7	990.59	—
8	979.29	—
9	826.10	—
10	620.45	—
11	233.87	—
12	—	108.85
Whole year	5517.5	540.2
Unbalance	90.2%	

It can be seen in Table 9 that the building structure can affect the heating and cooling load a little due to their insolation and heat conductivity difference, but the ambient temperature is the determine factor. The unbalance rate of Trondheim cases can be over 90% with solo CO<sub>2</sub> GSHP, causing soil temperature to reduce enormously.

Table 10 is the monthly energy loads when using a solo CO<sub>2</sub> ground source heat pump in Shanghai, China. It displays a different pattern from results in Harbin and Trondheim. With hot summer and relatively moderate winter, Shanghai suffers higher cooling load than heating load. The unbalance rate is 29.5% and it will cause soil temperature to go up.

Table 11 displays the monthly energy loads when using a solo CO<sub>2</sub> ground source heat pump in Guangzhou, China. Guangzhou is more like opposite version of Trondheim in China, long summer and warm spring and autumn make Guangzhou cooling dominate city and without other assistance, the soil unbalance rate can be 90.2%.



### 7.3 Simulation and analysis for solar assisted R744 GSHP without heat injection

In this part, solar assisted R744 GSHP without heat injection in summer is discussed. Harbin and Trondheim as the chosen typical cold winter climate cites were studied.

#### 7.3.1 Simulation and analysis for Harbin’s case

Fig. 17 below shows the performance of solar assisted ground source heat pump with the solar collector area change in winter.

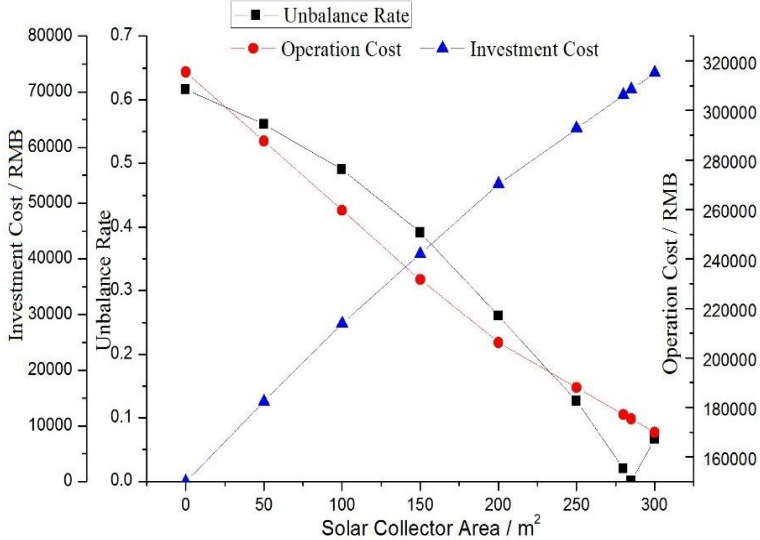


**Fig. 17 Performance of SAGSHP in Harbin (without heat injection)**

There are three lines using different Y axis in this figure, representing results of unbalance rate, annual operation cost and solar collector investment cost respectively. The black line with square dots indicates the unbalance rate change, it can be seen that with the enlargement of solar collector area, unbalance rate decrease accordingly. This is because the solar collected energy undertakes part of the heating load in the system, the larger solar collector gets, the more energy was supplied by the sun rather than soil. With this trend, when the solar collector area becomes 285.5 m<sup>2</sup>, the unbalance rate will be 0.03%, small enough to be ignored. Since the solar collector reduces heat pump load, the power needed for heat pump is lower as the solar collector area is bigger. So in the figure, the red line with round spots shows the same trend with the black line. The red line indicates the change of annual

operation cost. The blue line with triangle spots represents for investment cost of solar collector. It is obvious that with larger solar collector, the investment cost is higher. Even though the acceleration becomes milder with increasing of solar collector area, it is easy to notice that solar collector is quite expensive. When the solar collector is too large, the money saved by it would not be able to make up to the investment cost. This would cause the payback period to be too long to promote the system to utilization.

**7.3.2 Simulation and analysis for Trondheim’s case**

Fig. 18 below shows the performance of solar assisted ground source heat pump with the solar collector area change in winter.

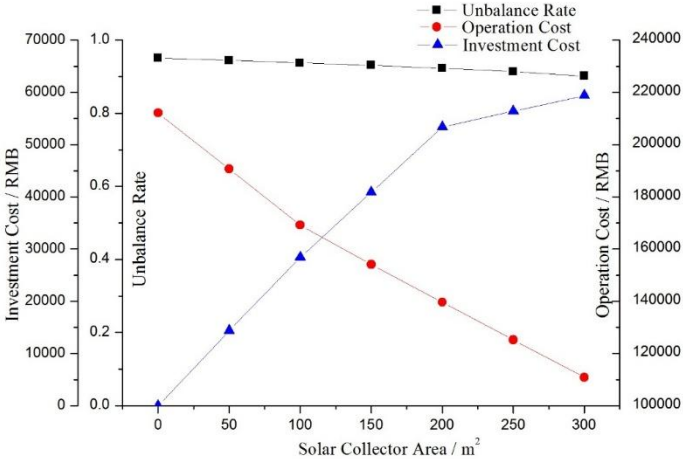


**Fig. 18 Performance of SAGSHP in Trondheim (without heat injection, Norwegian style)**

Like Fig. 17, there are three lines using different Y axis in this figure, representing results of unbalance rate, annual operation cost and solar collector investment cost respectively. These two figures share the same properties, without the detailed data, the two figures look very alike. The larger solar collector gets, the more energy was supplied by the sun rather than soil, so the unbalance rate will be smaller with the gaining of solar collector area. However, the unbalance rate in Trondheim is bigger than that in Harbin, and the solar radiation in Trondheim in winter is lower than that in Harbin, resulting from its short sunshine time. So different from the results in Harbin, with less than 300 m<sup>2</sup> of solar collector, there is no balance for heating and cooling heat transfer between underground heat exchanger and the soil. Of course if the solar collector continues to become bigger, at some point, which is 3500

m<sup>2</sup>, the heat extracted from the soil and heat released to soil will balance, but that would require large area of solar collector. This way is not economic and thus not approval by the industry and customer. The Chinese style building in Trondheim suffers from the same problem, here will not give the detailed data and figures.

In sum, resulting from short sunshine time and low temperature in winter, solar assistant ground source heat pump in Harbin and Trondheim is not ideal in operation. In Harbin, the unbalance rate can be reduced to 0.03% but it requires solar collector as large as 285.5 m<sup>2</sup>. This large solar collecting system costs more than what it's worth considering the money saved by collected solar energy. And this system does not work well in area with very high unbalance rate and very short sunshine time in winter like Trondheim, Norway. There should be another way to use more of the solar energy not only in winter but also in summer to overcome the difficulties.

## **7.4 Simulation and analysis for solar assisted R744 GSHP with heat injection**

In this part, solar assisted R744 GSHP with heat injection in summer is discussed. Harbin and Trondheim as the chosen typical cold winter climate cites were studied.

### **7.4.1 Simulation and analysis for Harbin's case**

Fig. 19 below shows the performance of solar assisted ground source heat pump with the solar collector area change in winter. When saying "with injection", it refers to the "charging mode" mentioned in section 4 that when summer solar energy is collected, this part of heat goes to soil and compensate part of lost heat in soil during winter. In this way, solar energy helps the soil temperature to maintain the same after one year's operation.

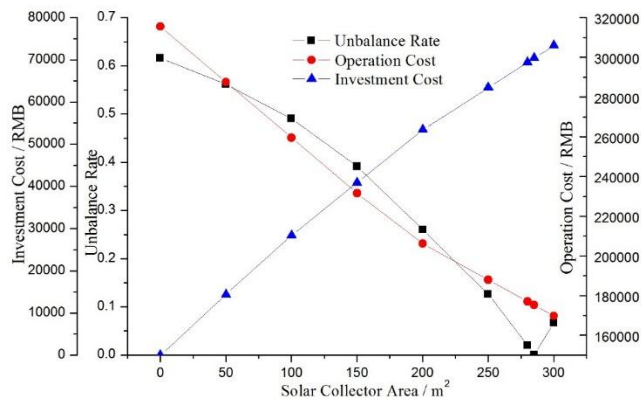


**Fig. 19 Performance of SAGSHP in Harbin (with heat injection)**

There are three lines using different Y axis in this figure, representing results of unbalance rate, annual operation cost and solar collector investment cost respectively. The black line with square dots indicates the unbalance rate change, it can be seen that with the enlargement of solar collector area, unbalance rate decrease accordingly. But when the solar collector area reaches some value, in this case, 122.5 m<sup>2</sup>, the unbalance rate starts to grow bigger again. This is because with larger solar collecting area, more energy is gained both in summer and in winter. In winter, it reduces the heating load from the ground source heat pump so that less heat is absorbed from the soil. In summer, more heat is release back to soil, it causes the soil temperature to go higher. In the both ways, when the solar collector is too large, the heat injected to soil becomes larger rather than smaller than that extracted from the soil, which is also not so good. So the recommended choice for this case is that solar collector area should be 122.5 m<sup>2</sup>.

The red line with round spots indicates the change of annual operation cost. The blue line with triangle spots indicates the change of investment cost. When the unbalance rate reaches almost 0%, the red lines displays a quite low value, it has reduced for almost 100,000 NOK. On the other hand, the investment cost is not that high, it is around 1000 NOK. Considering those two influencing factors, the solar collector area of 122.5 m<sup>2</sup> is still recommended.

Fig. 20 below shows the load bore by solar collecting system and underground heat exchangers when solar collector area is 122.5 m<sup>2</sup>. It can be seen that in May and September, solar collector is able to supply all the heating load the building needs, and in winter, it helps to reduce the heat transfer amount between soil and underground heat exchanger.

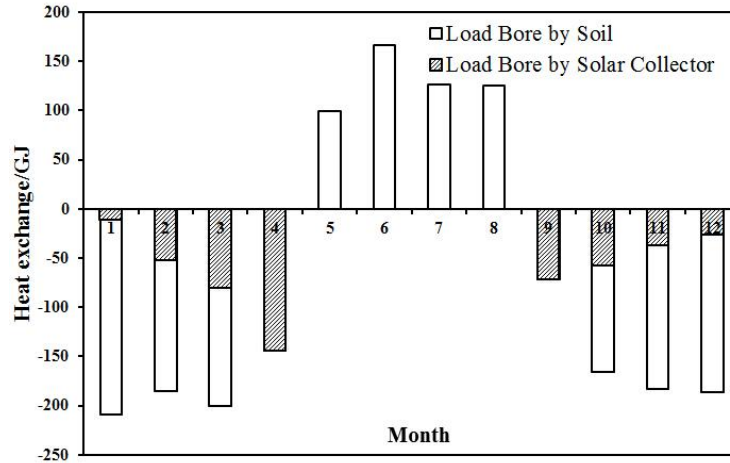


**Fig. 20 Heat exchange distribution with SAGSHP in Harbin**

### 7.4.2 Simulation and analysis for Trondheim’s case

Fig. 21 below shows the performance of solar assisted ground source heat pump with the solar collector area change in winter in Trondheim with Norwegian style structure.

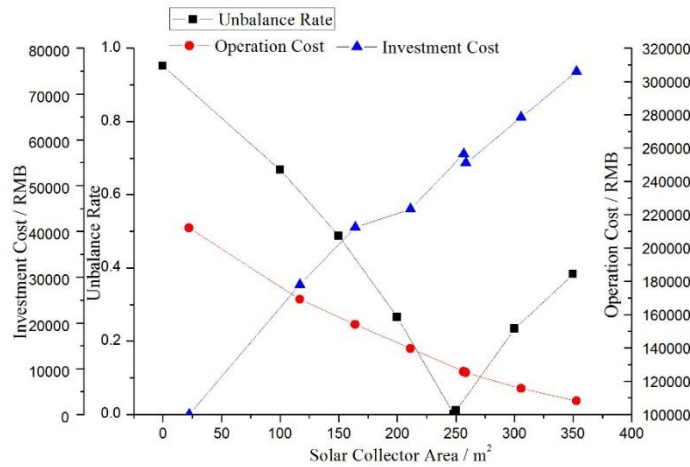


**Fig. 21 Performance of SAGSHP in Trondheim (with heat injection, Norwegian structure)**

Fig. 22 below shows the performance of solar assisted ground source heat pump with the solar collector area change in winter in Trondheim with Chinese style structure.

The black line with square dots indicates the unbalance rate change, it can be seen that with the enlargement of solar collector area, unbalance rate decrease accordingly like the case in Harbin. When the solar collector area reaches some value, in Norwegian structure case, 248.1 m<sup>2</sup>, in Chinese structure case, 241.8 m<sup>2</sup>, the unbalance rate starts to grow bigger again. So the recommended choice for this case is that solar collector area should be 248.1 m<sup>2</sup> and

241.8 m<sup>2</sup> respectively.

The annual operation cost red line and the change of investment cost blue line show the same trend in these two figures as well as in Harbin case. This is because all the cases share the same working principal, and it also shows the model is universal and predictive. Even though with different cases the accurate numerical values of results are not the same, but the regular pattern is the same and can be used to guide to individual recommended value from case to case.

These two figures show the same characteristics in the three lines on the figure though they share different detailed data. In Norwegian style building, the recommended solar collector area is 248.1 m<sup>2</sup> whereas the recommended solar collector area is 241.8 m<sup>2</sup>.

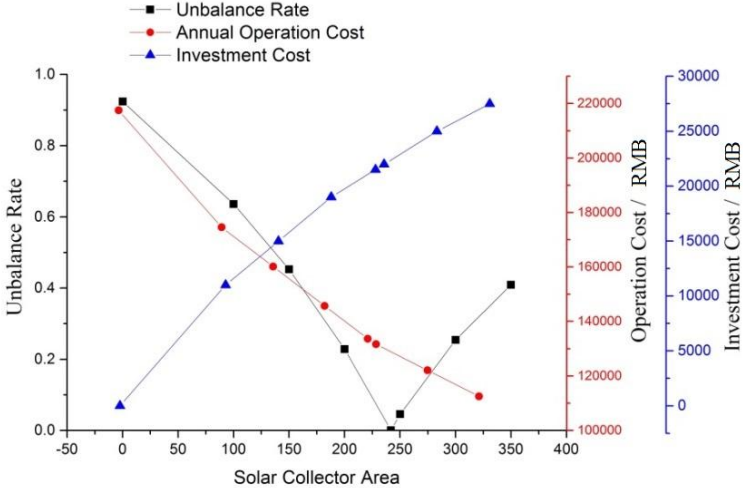
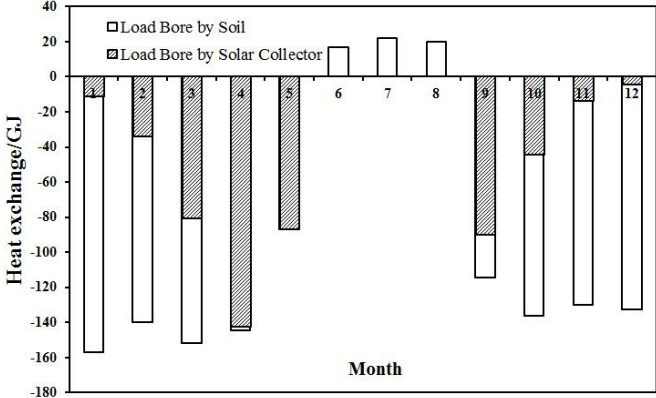


**Fig. 22 Performance of SAGSHP in Trondheim (with heat injection, Chinese structure)**

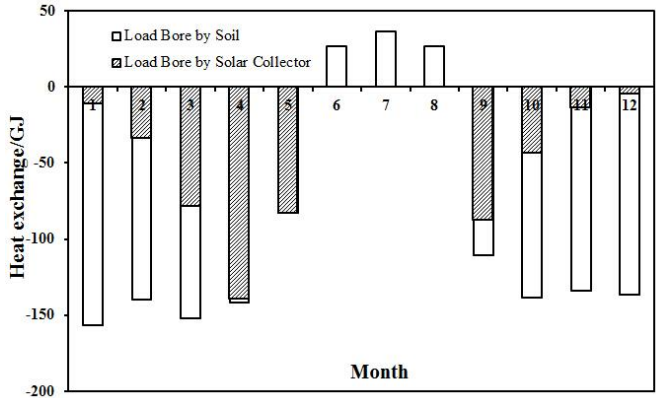
The differences in these two figures indicate that the building structure has its influence on the power needed for air conditioning system, but the difference is not large enough to be conclusive. Like in this case, the solar collector area is influenced by structure, causing a difference of almost 7 m<sup>2</sup> area. The operation cost is a little bit higher in Chinese structure building than that in Norwegian structure building, but the difference is too small for the total amount of cost to be reflected in the figures.

Fig. 23 and Fig. 24 below shows the load bore by solar collecting system and underground heat exchangers when solar collector area is 248.1 m<sup>2</sup> in Norwegian construction style building in Trondheim and solar collector area is 241.8 m<sup>2</sup> in Chinese construction style building in Trondheim respectively.

It can be seen from those two figures that the solar energy collected in April and May can almost cover all the heating need in the building. In September, the solar energy can also cover quite some. But since in section 8.3 shows, only using solar energy assistance in winter is not going to eliminate the unbalance situation completely, the heat injection from solar collecting system to soil is crucial to the novel system.



**Fig. 23 Heat exchange distribution with SAGSHP in Trondheim (Norwegian structure)**



**Fig. 24 Heat exchange distribution with SAGSHP in Trondheim (Chinese structure)**

**7.5 Simulation and analysis for R744 GSHP with air cooled gas cooler**

In this part, R744 GSHP with air cooled gas cooler is discussed. Shanghai and Guangzhou as the chosen typical hot summer climate cites were studied.

**7.5.1 Simulation and analysis for Shanghai’s case**

Fig. 25 below shows the performance of ground source heat pump system with air

cooled gas cooler based on how much heat is released to air and how much is released to the soil. The air cooled gas cooler and the heat pump system is coupled working, meaning when the cooling load reaches to some value, the air cooled gas cooler starts working, it releases part of the heat to the air. This value decides the percentage of load that is bore by the air cooled gas cooler. When this percentage changes, the unbalance rate, annual operation cost and investment cost changes.

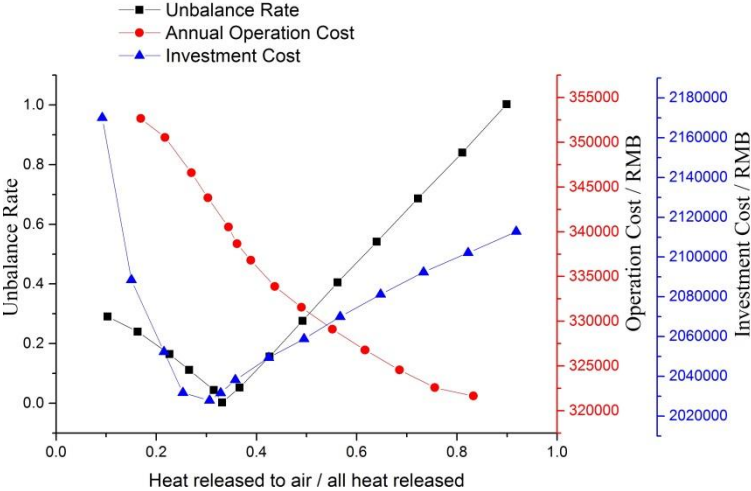


**Fig. 25 Performance of GSHP with gals cooler in Shanghai**

There are three lines using different Y axis in this figure, representing results of unbalance rate, annual operation cost and solar collector investment cost respectively. Just like the figures above, the black line with square dots indicates the values of unbalance rate, the red line with round spots indicates the values of annual operation cost in RMB and the blue line with triangle dots indicates the values of investment cost. Different with solar assisted ground source heat pump system, the investment cost here indicates the cost for the whole system, while the investment cost in figures above indicates the cost of solar collecting system.

The unbalance rate value changes as the percentage of heat released by air cooled gas cooler changes. While the percentage becomes larger, the unbalance rate first decreases for some time and then starts to increase. It can be seen from the figure that when air cooled gas cooler bears 29.5% of all the heat released by the heat pump system, the unbalance rate can be reduced to 0%. This is because with the increasing of the percentage, more and more heat is released to the atmosphere. At first this situation helps shorten the difference between the heat



released to soil and heat gained from soil of GSHP system, but when the percentage keeps going higher, the heat release to soil is smaller than that gained from soil annually, the unbalance rate starts to grow, just to the other direction.

It is interesting to see that the line of investment cost keeps a similar pattern as the line of unbalance rate. This is because unlike SAGSHP, using air cooled gas cooler can reduce the underground heat exchanger investment, thus the initial cost of system is reduced. However, the cost of air source gas cooler goes higher with its larger burden, so when it reaches to a certain value, the investment cost starts to grow and finally it will be more expensive than a solo ground source heat pump.

The operation cost line shows the trend of going lower continuously. This is because the burden of heat pump system is quite relieved by air source gas cooler, the power needed for the system keeps going lower.

Fig. 26 below shows the load distribution in GSHP with air cooler gas cooler in Shanghai when the recommended percentage 29.5% is chosen.

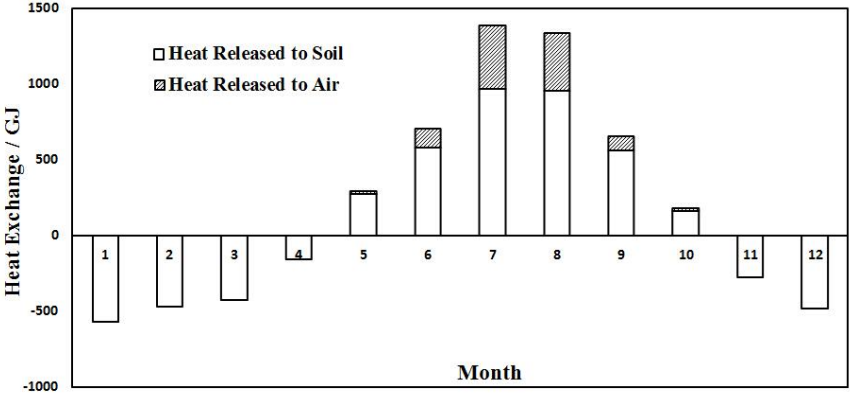


**Fig. 26 Heat exchange distribution of GSHP with air cooled gas cooler in Shanghai**

Fig. 26 also shows that the burden of ground source heat pump is shared, the power consumption is less than before and more importantly, the balance of heat in soil after annual operation is reached. Table 14 below shows the performance comparison between solo R744 GSHP and R744 GSHP with air source gas cooler in detail. The reduction in unbalance rate, ground heat exchanger max cooling load, total operation power and operation cost is clear in this table.

**Table 12 Comparisons of operation in solo GSHP and GSHP with air source gas cooler**

City	Operation Type	GHX	GHX	Unbalance	GHX Max	GHX Max	Total	Total load	Operation cost
		cooling	heating		Cooling	Heating	Operation		
		load	load		Load	Load	Power		
		GJ	GJ		kW	kW	GJ	GJ	RMB
Shanghai	Solo	3445.5	2430.6	29.5%	545.6	238.0	2096.143	5876	355180
	Coupled	2430.6	2430.6	0	212.8	238.0	1871.428		317103

Due to the reduction in ground heat exchanger max cooling load, the investment cost can be reduced, also as shown in Fig. 25. The detailed information is given in Table 15.

**Table 13 Comparisons of investment in solo GSHP and GSHP with air source gas cooler**

Investment	R744 Ground source heat	R744 heat pump with coupled operation of ground
X10 <sup>4</sup> RMB	pump	heat exchanger and air source gas cooler
Instrument	124.68	140.00
Transformer device	7.05	7.1
Installation	37.40	38.0
Natural Gas	0	0
Ground HX	134.40	58.63
Total	303.53	243.73

### 7.5.2 Simulation and analysis for Guangzhou's case

Fig. 27 below shows the performance of ground source heat pump system with air cooled gas cooler based on how much heat is released to air and how much is released to the soil. The air source bear load proportion decides the unbalance rate, the operation cost and the investment cost. When this percentage changes, these parameters change as in the case in Shanghai.

There are also three lines using different Y axis in this figure, representing results of unbalance rate, annual operation cost and solar collector investment cost respectively. Each line represents the same parameter in this figure as in all the figures above.

It can be seen from the figure that when air cooled gas cooler bears 90% of all the heat released by the heat pump system, the unbalance rate can be reduced to 0%.

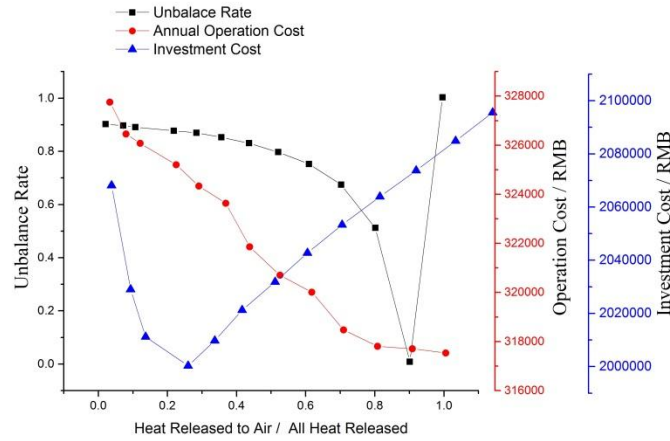


**Fig. 27 Performance of GSHP with gas cooler in Guangzhou**

The investment cost line shows the same pattern as the line in Shanghai case, it stops going down and starts going high at the proportion around 28%. Suffering from the long and high temperature summer, Guangzhou needs the air source gas cooler to take over much more heat than it is needed in Shanghai case. So, the number of gas cooler needed increase, along with the investment cost. Even though the investment cost is not lower than the solo ground source heat pump system, this novel system with air source gas cooler still shows more advantage due to its low operational cost and good ability to maintain heat balance in the soil.

The performance comparison between solo R744 GSHP and R744 GSHP with air source gas cooler in Guangzhou is shown in Table 16 in detail. The reduction in unbalance rate, ground heat exchanger max cooling load, total operation power and operation cost is clear in this table.

**Table 14 Comparisons of operation in solo GSHP and GSHP with air source gas cooler**

City	Operation Type	GHX	GHX	Unbalance	GHX Max	GHX Max	Total Operation Power	Total load	Operation cost	
		cooling load	heating load		Cooling Load	Heating Load				
		GJ	GJ			kW	kW	GJ	GJ	RMB
Guangzhou	Solo	5517.5	540.2	90%	554.4	221.2	2007.713	6057	340196	
	Coupled	540.2	540.2	0	27.4	221.2	1949.202		330281	

## 8. Conclusion

In this thesis, a solar assistant ground source heat pump with air source gas cooler is simulated and analyzed. Numerical models of each component is developed and validated by experimental data from existing literature. After analyzing the simulated results of the whole system in four typical cites, the conclusions of this thesis are given:

- 1) Solo R744 ground source heat pump operation can cause high unbalance rate in area without moderate climate. The unbalance rates in Harbin, Trondheim(Norwegian structure), Trondheim(Chinese structure), Shanghai and Guangzhou are 61.6%, 95.1%, 92.4%, 29.5% and 90.2% respectively;
- 2) Without heat injection to soil in summer, solar assistance in winter only can reduce limited unbalance rate with same solar collector area. When the unbalance rate is very high, using solar collector in winter only to erase unbalance rate is costly. With heat injection to soil in summer, solar assistance is of greater help for eliminating heat unbalance after annual operation. In the case in Harbin, the solar collector area needed to balance heat reduced by 57%;
- 3) There can be found an optimized solar collector area in the cases, for Trondheim with Norwegian structure, the optimized solar collector area is 248.1m<sup>2</sup>, for Trondheim with Chinese structure, the optimized solar collector area is 241.8m<sup>2</sup>. Solar collector undertakes 43.37% of the total burden, for Harbin the optimized solar collector area is 122.5 m<sup>2</sup>. Solar collector undertakes 25.73% of the total energy load.
- 4) Air source gas cooler can efficiently help the R744 ground source heat pump reduce the unbalance rate in cold winter climate area compared to using solo R744 ground source heat pump. As the proportion of air source bearing load goes higher, the investment cost first goes down and then when the proportion is around 28%, it goes up;
- 5) As the proportion of air source bearing load goes higher, the operation cost goes down continuously. There is an optimized proportion of air source cooling load in

cases. For Shanghai the proportion is 29.5%, the unbalance rate is 0%. For Guangzhou the proportion is 90%, the unbalance rate is 0%.

- 6) In Shanghai case, when unbalance rate is 0%, the operation cost is 23% lower and the investment cost is 20% lower than that of solo R744 GSHP system;

## **9. Proposal for further work**

After the work in this thesis, some problems are solved but not entirely satisfying, the proposal for further work of this thesis is given below:

- 1) The model should be built into experimental units and validated by the whole system experimental data;
- 2) The heat injection to the soil should consider more about heat storage underground.

## Reference

- [1] Omer A. M, Energy environment and sustainable development. *Renew Sustain Energy Rev* 2007.
- [2] H Yang, P Cui, Z Fang. 2010, Vertical-borehole ground-coupled heat pumps: a review of models and systems, *Applied Energy*, 87(1):16-27.
- [3] Yaodong H, Zhen M, Core of long-term effective development of ground source heat pump-dynamic heat balance of rock and soil between summer and winter (in Chinese), *Heat Ventilation Air Condition* 39 (2009) 74-76.
- [4] X.Q.Zhai, X.L.Wang, H.T. Pei, Y.Yang, R.Z.Wang, Experimental investigation and optimization of a ground source heat pump system under different indoor set temperatures, *Applied Thermal Engineering* 48 (2012) 105-116.
- [5] Huajun W, Chengying Q, Enyu W, Jun Z, A case study of underground thermal storage in a solar-ground coupled heat pump system for residential buildings, *Renewable Energy* 34 (2009) 307-314.
- [6] Catherine S. Norman, Stephen J. DeCanio, Lin Fan, The Montreal Protocol at 20: Ongoing opportunities for integration with climate protection, *Global Environmental Change* 18 (2008) 330-340.
- [7] Brian T. Austin, K. Sumathy, Parametric study on the performance of a direct-expansion geothermal heat pump using carbon dioxide. *Applied Thermal Engineering* 31 (2011) 3774-3782.
- [8] Brian T. A, Sumathy K, Parametric study on the performance of a direct-expansion geothermal heat pump using carbon dioxide, *Applied Thermal Engineering* 31 (2011) 3774-3782.
- [9] Antonio C, Michele De C, Angelo Z, Design of borehole heat exchangers for ground-source heat pumps: A literature review, methodology comparison and analysis on the penalty temperature, *Energy and Buildings* 55 (2012) 369–379.
- [10] A. Pearson, Carbon dioxide-new uses for an old refrigerant, *International Journal of*

Refrigerant 28 (2005) 1140-1148.

[11] W. S. Bodinus, The rise and fall of carbon dioxide systems, ASHRAE Journal 4 (1999) 37-42.

[12] P. Neks & H. T. Walnum, A. Hafner, CO<sub>2</sub>- A refrigerant from the past with prospects of being one of the main refrigerants in the future. 9th IIR Gustav Lorentzen conference 2010-natural refrigerants-real alternatives, Sydney, April 12-14, 2010.

[13] Lorentzen G. 1990, Trans-critical vapor compression cycle device. Patent WO/07683.

[14] Pearson S F. Cooling system incorporating a secondary heat transfer circuit: U.S. Patent 5,400,615[P]. 1995-3-28.

[15] G Lorentzen, J Pettersen. A new, efficient and environmentally benign system for car air-conditioning, International Journal of Refrigeration, 1993 (16): 4-12.

[16] P. Neks & The transcritical vapor compression cycle. Its potential in heat pump processes, Refrigeration, Energy and Environment Int. Symposium on the 40th Anniversary of NTH Refrigeration Engineering, Trondheim, June 22-24, 1992.

[17] Sergio Giroto, Silvia Minetto, Petter Neks & Commercial refrigeration system using CO<sub>2</sub> as the refrigerant, International Journal of Refrigeration 27 (2004) 717-723.

[18] Schiefloe PA, Neks & P. CO<sub>2</sub> varmepumpe for bygning-soppvarming, forprosjekt (in Norwegian). SINTEF Report. Trondheim, SINTEF Energy Research, 1999.

[19] P. Bansal, A review-Status of CO<sub>2</sub> as a low temperature refrigerant: Fundamentals and R&D opportunities, Applied Thermal Engineering 41 (2012) 18-29.

[20] Z.H. Ayub, Recent developments in CO<sub>2</sub> heat transfer, Heat Transfer Engineering 26 (6) (2005) 3-6.

[21] M.H. Kim, J. Pettersen, C. Bullard, Fundamental process and system design issues in CO<sub>2</sub> vapor compression systems, Progress in Energy and Combustion Science 30 (2004) 119-174.

[22] S.M. Liao, T.S. Zhao, Measurements of heat transfer coefficients from supercritical carbon dioxide flowing in horizontal Mini/Micro Channels, Journal of Heat Transfer-Transactions of the ASME 123 (2002) 413-420.

[23] Span, R, and W. Wagner, A New Equation of State for Carbon Dioxide Covering the Fluid Region from the Triple-Point Temperature to 1100 K at Pressures up to 800 MPa, Journal of Physical and Chemical Reference Data 25(6) (1996) 1509-1596.

[24] Vesovic, V., W.A. Wakeham, G.A. Olchowky, J.V. Sengers, J.T.R. Watson, and J. Millat, The



Transport Properties of Carbon Dioxide, Journal Physical Chemical Reference Data 19 (3) (1990) 763 –808.

[25] Srinivas S. Pitla , Douglas M. Robinson , Eckhard A. Groll and Satish Ramadhyani, Heat transfer from supercritical carbon dioxide in tube flow: a critical review, HVAC&R RESEARCH, 4 (3) (1998) 281-301.

[26] Klein, S.A, Engineering Equation Solver (EES), Madison, WI: F-Chart Software, (2004).

[27] Eckhard A. Groll, Jun-Hyeung Kim, Review article: Review of recent advances toward transcritical CO<sub>2</sub> cycle technology, HVAC & R Research 13 (2007) 499-520.

[28] A. Fartaj, D. S.-K. Ting, W. W. Yang, Second law analysis of the transcritical CO<sub>2</sub> refrigeration cycle, Energy Conversion and Management 45 (2004) 2269-2281.

[29] S.G. Kim, Y.J. Kim, G. Lee, M.S. Kim, The performance of a transcritical CO<sub>2</sub> cycle with an internal heat exchanger for hot water heating, International Journal of Refrigeration 28 (2005) 1064-1072.

[30] R. Cabello, D. Sánchez, J. Patiño, R. Llopis, E. Torrella, Experimental analysis of energy performance of modified single-stage CO<sub>2</sub> transcritical vapour compression cycles based on vapour injection in the suction line, Applied Thermal Engineering 47 (2012) 86-94.

[31] Xiaohan Jia, Bo Zhang, Lei Pu, Bei Guo, Xueyuan Peng, Improved rotary vane expander for trans-critical CO<sub>2</sub> cycle by introducing high-pressure gas into the vane slots, International Journal of Refrigeration 34 (2011) 732-741.

[32] Jahar Sarkar, Cycle parameter optimization of vortex tube expansion transcritical CO<sub>2</sub> system, International Journal of Thermal Sciences 48 (2009) 1823–1828.

[33] Daqing Li, Eckhard A. Groll, Transcritical CO<sub>2</sub> refrigeration cycle with ejector-expansion device, International Journal of Refrigeration 28 (2005) 766-773.

[34] Jahar Sarkar, Optimization of ejector-expansion transcritical CO<sub>2</sub> heat pump cycle, Energy 33 (2008) 1399-1406.

[35] Sun Fangtian, Ma Yitai, Thermodynamic analysis of transcritical CO<sub>2</sub> refrigeration cycle with an ejector, Applied Thermal Engineering 31 (2011) 1184-1189.

[36] Jiwen Cen, Pei Liu, Fangming Jiang, A novel transcritical CO<sub>2</sub> refrigeration cycle with two ejectors, International Journal of Refrigeration 35 (2012)2233-2239.

[37] Masafumi Nakagawa, Ariel R. Marasigan, Takanori Matsukawa, Experimental analysis on the effect of internal heat exchanger in transcritical CO<sub>2</sub> refrigeration cycle with two-phase ejector, International Journal of Refrigeration 34(2011)1577-1586.

- [38] Zhen-ying Zhang, Yi-tai Ma, Hong-li Wang, Min-xia Li, Theoretical evaluation on effect of internal heat exchanger in ejector expansion transcritical CO<sub>2</sub> refrigeration cycle, *Applied Thermal Engineering* 50 (2013) 932-938.
- [39] Alberto Cavallini, Luca Cecchinato, Marco Corradi, Ezio Fornasieri, Claudio Zilio, Two-stage transcritical carbon dioxide cycle optimisation: A theoretical and experimental analysis, *International Journal of Refrigeration* 28 (2005) 1274-1283.
- [40] Neeraj Agrawal, Souvik Bhattacharyya, J. Sarkar, Optimization of two-stage transcritical carbon dioxide heat pump cycles, *International Journal of Thermal Sciences* 46 (2007) 180-187.
- [41] Luca Cecchinato, Manuel Chiarello, Marco Corradi, Ezio Fornasieri, Silvia Minetto, Paolo Stringari, Claudio Zilio, Thermodynamic analysis of different two-stage transcritical carbon dioxide cycles, *International Journal of Refrigeration* 32(2009)1058-1067.
- [42] Friedrich KauP, Determination of the optimum high pressure for transcritical CO<sub>2</sub>-refrigeration cycles. *International Journal Thermal Science*. (1999) 38, 325-330.
- [43] S.M. Liao, T.S. Zhao, A. Jakobsen, A correlation of optimal heat rejection pressures in transcritical carbon dioxide cycles, *Applied Thermal Engineering* 20 (2000) 831-841.
- [44] J. Sarkar, S. Bhattacharyya, M. R. Gopal, Optimization of a transcritical CO<sub>2</sub> heat pump cycle for simultaneous cooling and heating applications, *International Journal of Refrigeration* 27 (2004) 830-838.
- [45] Petter Neks & CO<sub>2</sub> heat pump systems, *International Journal of Refrigeration* 25 (2002) 421-427.
- [46] Petter Neks & Rune L. Hoggen, Kåre Aflekt, Arne Jakobsen, Geir Skaugen, Fan-less heat exchanger concept for CO<sub>2</sub> heat pump systems, *International Journal of Refrigeration* 28 (2005) 1205–1211.
- [47] J. Sarkar, Souvik Bhattacharyya, M. Ram Gopal, Simulation of a transcritical CO<sub>2</sub> heat pump cycle for simultaneous cooling and heating applications, *International Journal of Refrigeration* 29 (2006) 735–743.
- [48] Neeraj Agrawal, Souvik Bhattacharyya, Studies on a two-stage transcritical carbon dioxide heat pump cycle with flash intercooling, *Applied Thermal Engineering* 27 (2007) 299-305.
- [49] Xiao Xiao Xu, Guang Ming Chen, Li Ming Tang, Zhi Jiang Zhu, Experimental investigation on performance of transcritical CO<sub>2</sub> heat pump system with ejector under optimum high-side pressure, *Energy* 44 (2012) 870-877.

- [50] Brian T. Austin and K. Sumathy, Parametric study on the performance of a direct-expansion geothermal heat pump using carbon dioxide, *Applied Thermal Engineering* 31 (2011) 3774-3782.
- <sup>51</sup> Young-Jae Kim, Keun-Sun Chang, Development of a thermodynamic performance-analysis program for CO<sub>2</sub> geothermal heat pump system, *Journal of Industrial and Engineering Chemistry* 19 (2013) 1827–1837.
- [52] Petter Neks å Håvard Rekstad, G. Reza Zakeri and Per Arne Schiefloe, CO<sub>2</sub>-heat pump water heater: characteristics, system design and experimental results. *International Journal of Refrigeration*, 21 (3) (1998) 172-179.
- [53] K.Kaygusuz, Performance of solar-assisted heat pump systems, *Applied Energy* 51 (1995) 93-109.
- [54] G.Panaras, E.Mathioulakis, V.Belessiois, Investigation of the performance of a combined solar thermal heat pump hot water system, *Solar Energy* 93 (2013) 169-182.
- [55] S.Deng, Y.J.Dai, R.Z.Wang, T.Matsuura, Y.Yasui, Comparison study on performance of a hybrid solar-assisted CO<sub>2</sub> heat pump, *Applied Thermal Engineering* 31 (2011) 3696-3705.
- [56] S.Taira, H.Nakayama, E.Kumakura, The development of heat pump water heaters using CO<sub>2</sub> refrigerant, in: 2010 International Symposium on Next-generation Air Conditioning and Refrigeration Technology, Tokyo, Japan (2010).
- [57] O.Ozgener, A.Hepbasli, A review on the energy and exergy analysis of solar assisted heat pump systems, *Renewable and Sustainable Energy Reviews* 11 (2007) 482-496.
- [58] F.M.Rad, A.S.Fung, W.H.Leong, Feasibility of combined solar thermal and ground source heat pump systems in cold climate, Canada, *Energy and Buildings* 61 (2013) 224-232.
- [ 59 ] E.Wang, A.S.Fung, C.Qi, W.H.Leong, Performance prediction of a hybrid solar ground-source heat pump system, *Energy and Buildings* 47 (2012) 600-611.
- [60] T.M. Ortiz, D. Li, E.A. Groll, Evaluation of the performance potential of CO<sub>2</sub> as a refrigerant in air-to-air air conditioners and heat pumps: System modeling and analysis. ARTI, 2003, Final Report.
- [61] H. Blasius, *Das Ähnlichkeitsgesetz bei Reibungsvorgängen in Flüssigkeiten*, Springer Berlin Heidelberg, 1913.
- [62] B.T. Austin, K. Sumathy, Parametric study on the performance of a direct-expansion

geothermal heat pump using carbon dioxide, *Applied Thermal Engineering* 31 (2011) 3774-3782.

[63] H.Y. Zeng, N.R. Diao, Z.H. Fang, A finite line-source model for boreholes in geothermal heat exchangers, *Heat Transfer-Asian Research* 31 (2002) 558-567.

[64] H.Y. Zeng, Z.H. Fang, A mathematical model of axial fluid temperature for U tube geothermal heat exchangers (in Chinese), *J. Shandong Inst. Archit Eng.* 17 (2002) 7-11.

[65] H.Y. Zeng, N.R. Diao, Z.H. Fang, A quasi three dimensional heat transfer model for vertical U-tube geothermal heat exchangers, *J. Eng. Therm. Energ. Power* 18 (2003) 387-390.

[66] C.C. Wang, J.Y. Jang, N.F. Chiou, A heat transfer and friction correlation for wavy fin-and-tube heat exchangers, *Int. J. Heat and Mass Transfer* 42 (1999) 1919-1924.

[67] Pertzborn A, Hackel S, Nellis G, et al. Experimental validation of a ground heat exchanger model in a hybrid ground source heat pump[J]. *HVAC&R Research*, 2011, 17(6): 1101-1114.

[68] Hackel S, Pertzborn A. Effective design and operation of hybrid ground-source heat pumps: Three case studies[J]. *Energy and Buildings*, 2011, 43(12): 3497-3504.

[69] Zhai X Q, Wang X L, Pei H T, et al. Experimental investigation and optimization of a ground source heat pump system under different indoor set temperatures[J]. *Applied Thermal Engineering*, 2012, 48: 105-116.

[70] Carsen J. Banister, William R. Wager, Michael R. Collins. Validation of a single tank, multi-mode solar-assisted heat pump TRNSYS model, *Energy Procedia*, 48(2014): 499-504.